The arbuscular mycorrhizal fungus Rhizophagus irregularis uses the copper exporting ATPase RiCRD1 as a major strategy for copper detoxification

Tamara Gómez-Gallego, Ma Jesús Molina-Luzón, Genevieve Conéjéro, Pierre Berthomieu, Nuria Ferrol

Journal Pre-proof

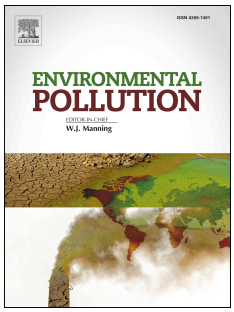

The arbuscular mycorrhizal fungus *Rhizophagus irregularis* uses the copper exporting ATPase RiCRD1 as a major strategy for copper detoxification

Tamara Gómez-Gallego, M[a] Jesús Molina-Luzón, Genevieve Conéjéro, Pierre Berthomieu, Nuria Ferrol

PII: S0269-7491(23)01992-9

DOI: https://doi.org/10.1016/j.envpol.2023.122990

Reference: ENPO 122990

To appear in: *Environmental Pollution*

Received Date: 25 May 2023

Revised Date: 10 November 2023

Accepted Date: 16 November 2023

Please cite this article as: Gómez-Gallego, T., Molina-Luzón, Ma.Jesú., Conéjéro, G., Berthomieu, P., Ferrol, N., The arbuscular mycorrhizal fungus *Rhizophagus irregularis* uses the copper exporting ATPase RiCRD1 as a major strategy for copper detoxification, *Environmental Pollution* (2023), doi: https://doi.org/10.1016/j.envpol.2023.122990.

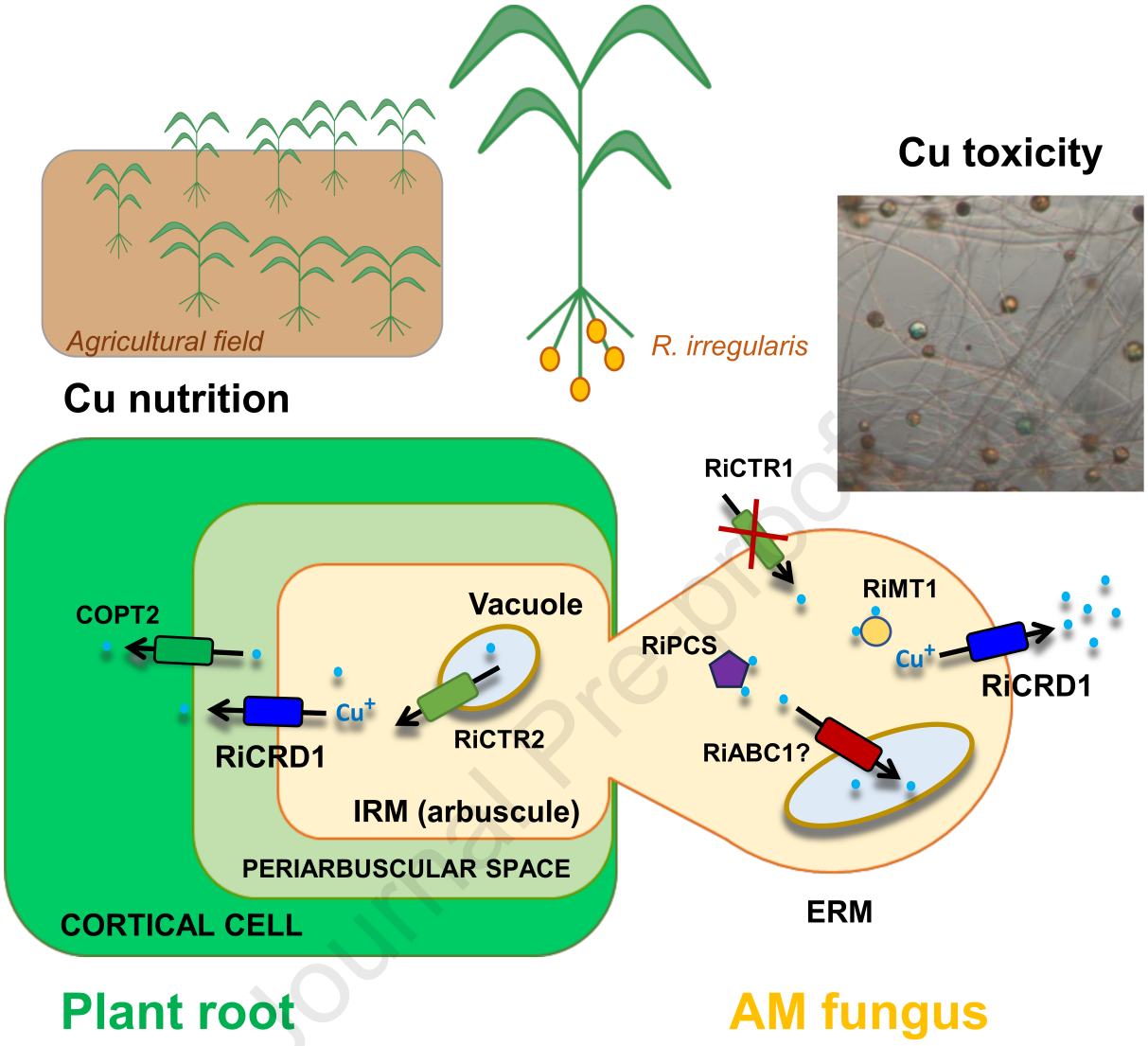

The arbuscular mycorrhizal fungus *Rhizophagus irregularis* uses the copper exporting ATPase RiCRD1 as a major strategy for copper detoxification

Tamara Gómez-Gallego[a], Mª Jesús Molina-Luzón[a], Genevieve Conéjéro[b], Pierre Berthomieu[b] and Nuria Ferrol[a*]

[a] *Soil and Plant Microbiology Department, Estación Experimental del Zaidín, Consejo Superior de Investigaciones Científicas, Granada, Spain*

[b] *Institut des Sciences des Plantes de Montpellier, Université de Montpellier, Centre National de la Recherche Scientifique, Institut Agro Montpellier, Institut National de Recherche pour l'Agriculture l'Alimentation et l'Environnement, Montpellier, France*

*Corresponding author:

E-mail address: nuria.ferrol@eez.csic.es (N. Ferrol)

Abstract

Arbuscular mycorrhizal (AM) fungi establish a mutualistic symbiosis with most land plants. AM fungi regulate plant copper (Cu) acquisition both in Cu deficient and polluted soils. Here, we report characterization of *RiCRD1*, a *Rhizophagus irregularis* gene putatively encoding a Cu transporting ATPase. Based on its sequence analysis, RiCRD1 was identified as a plasma membrane Cu^+ efflux protein of the P_{1B1}-ATPase subfamily. As revealed by heterologous complementation assays in yeast, *RiCRD1* encodes a functional protein capable of conferring increased tolerance against Cu. In the extraradical mycelium, *RiCRD1* expression was highly up-regulated in response to high concentrations of Cu in the medium. Comparison of the expression patterns of different players of metal tolerance in *R. irregularis* under high Cu levels suggests that this fungus could mainly use a metal efflux based-strategy to cope with Cu toxicity. *RiCRD1* was also expressed in the intraradical fungal structures and, more specifically, in the arbuscules, which suggests a role for RiCRD1 in Cu release from the fungus to the symbiotic interface. Overall, our results show that *RiCRD1* encodes a protein which could have a pivotal dual role in Cu homeostasis in *R. irregularis*, playing a role in Cu detoxification in the extraradical mycelium and in Cu transfer to the apoplast of the symbiotic interface in the arbuscules.

Keywords: arbuscular mycorrhiza; copper homeostais; *Rhizophagus irregularis*; heavy metal ATPase; metallothionein; phytochelatin synthase

Abbreviations: AM, arbuscular mycorrhiza; Cu, copper; ERM, extraradical mycelium; HMA, heavy metal ATPase; IRM, intraradical mycelium; PC, phytochelatin; PCS, phytochelatin synthase; ROS, reactive oxygen species

1. Introduction

Copper (Cu) homeostasis is tightly controlled in all organisms due to the dual effect of this transition metal. Cu is an essential micronutrient, but it is a toxic element when in excess. It is actively used as a cofactor by cytochrome *c* oxidases, superoxide dismutases and multicopper oxidases, among other enzymes that are involved in important processes such as respiration, reactive oxygen species (ROS) removal and Fe nutrition (Festa and Thiele, 2011; Linder, 1991). The key role of Cu in metabolic processes is associated with its ability to switch between an oxidized (Cu^{2+}) and a reduced (Cu^{+}) state, resulting in the acceptance and donation of single electrons in cellular redox reactions. However, these redox properties also make this metal toxic when present at high concentrations. Cu excess can damage DNA, proteins and lipids through the generation of ROS by Fenton like reactions. It can also displace other metal cofactors such as iron and zinc (Halliwell and Gutteridge, 1984; Macomber and Imlay, 2009).

Although Cu is a trace element, Cu toxicity has become an agricultural and environmental problem for decades owing mainly to anthropogenic activities. High Cu concentrations are toxic to soil inhabitants. However, some soil microorganisms have developed adaptative mechanisms that allow them to survive and grow in environments with high Cu concentrations (Bååth, 1989; Ferrol *et al*., 2009). Arbuscular mycorrhizal (AM) fungi, obligate biotrophs of higher plants, constitute one of the most prominent groups of soil microorganisms (Pozo *et al*., 2021; Shi *et al.*, 2023). AM fungi belong to the subphylum Glomeromycotina within the phylum Mucoromycota and establish a widespread mutualistic symbiosis with most land plants (Brundrett and Tedersoo, 2018; Spatafora *et al*., 2016). The fungus biotrophically colonizes the root cortex and develops

specialized structures, the arbuscules, to facilitate nutrient exchanges between symbionts (Luginbuehl and Oldroyd, 2017). Simultaneously, the fungus develops an extensive network of extraradical hyphae that can absorb nutrients beyond the depletion zone that develops around the roots, providing a new pathway, the mycorrhizal pathway, for the uptake of low mobility macronutrients, such as phosphorus, and micronutrients (Cu, Zn) in soil (Coccina et al., 2019; Lanfranco *et al*., 2018; Moreno Jiménez *et al.*, 2023; Wipf *et al*., 2019). In return, the AM fungus receives up to 20 % of the photosynthetically fixed carbon from the plant in the form of lipids and sugars (An *et al.*, 2019; Brands and Dörman 2022; Jiang *et al.*, 2017; Roth and Paszkowski, 2017). Mechanisms of phosphorus and nitrogen transport through the mycorrhizal pathway have been widely studied (Ferrol *et al*., 2019; Hui *et al.*, 2022; Wang *et al*., 2020; Xie *et al.*, 2022), but little is known about the components involved in micronutrient nutrition in AM associations (Ferrol *et al*., 2016; Ruytinx *et al*., 2020). As genetic manipulation of AM fungi remains challenging, the main advances have been performed on the host plant. In recent years functional analysis of AM fungal genes highly expressed in the intraradical mycelium has been achieved by using host-induced and virus-induced gene silencing strategies (Ezawa *et al.*, 2020; Helber *et al.*, 2011; Wang *et al.*, 2023). However, more studies are required to improve the applicability of these methodologies since their efficiency is unpredictable and gene and construct dependent (Hartmann et *al.*, 2020).

In soils with low Cu levels, the contribution of the mycorrhizal pathway to plant Cu nutrition can be up to 75% (Lee and George, 2005; Li *et al*., 1991). To our knowledge only two components of the mycorrhizal Cu uptake have been described so far: RiCTR1, a *Rhizophagus irregularis* plasma membrane Cu transporter of the CTR family whose expression in the extraradical mycelium (ERM) increases under Cu

deficiency but decreases under Cu toxicity (Gómez-Gallego *et al*., 2019), and *MtCOPT2*, a *Medicago truncatula* plasma membrane Cu transporter specifically expressed in arbuscule-colonized cortical root cells (Senovilla *et al*., 2020). However, it is currently unknown how Cu is released by the fungus to the apoplast of the symbiotic interface developed in the cortical cells colonized by arbuscules.

Under conditions of supraoptimal levels of Cu, AM fungi are able to alleviate metal toxicity in the plant. Different mechanisms have been proposed to explain the protective effect of the AM symbiosis under heavy metal stress (Ferrol *et al*., 2016; Gómez-Gallego *et al.* 2022; Shi *et al.* 2019). One of the mechanisms to mitigate the effect of Cu toxicity is the reduction of the effective concentration of metal available to the plant through immobilization of the metal in the intraradical and extraradical structures of the fungus (Cornejo *et al*., 2013; González-Guerrero *et al*., 2008). This is possible thanks to the existence in the fungus of a complex regulatory system that controls Cu homeostasis and avoids Cu stress in the cytosol. This system includes metal binding to the cell wall, reduction of metal uptake, intracellular buffering through the activity of intracellular chelators, such as metallothioneins and glutathione, and compartmentalization of Cu in vacuoles or spores (Ferrol *et al*., 2009; Ma *et al.*, 2022). However, a mechanism related to the control of Cu efflux has not been described yet.

Export of metal ions, such as Cu, Zn and Cd, usually takes place through P_{IB}-type ATPases, commonly known as HMAs (Heavy Metal ATPases). These proteins couple ATP hydrolysis to the transport of a heavy metal across cellular membranes in a multistep process, which includes the specific recognition of the metal (Palmgren and Nissen, 2011; Salustros *et al.* 2022). They possess six or eight transmembrane domains, a conserved intramembranous CPX signature needed for metal translocation, and cytoplasmic metal binding domains, which makes them different to their archetypal P-

ATPases counterparts (Arguello *et al*., 2007; Solioz and Vulpe, 1996). The genome of the model fungus *Rhizophagus irregularis* has four candidate genes putatively encoding P_{1B}-type ATPases (Tamayo *et al*., 2014). *RiCCC2.1*, *RiCCC2.2* and *RiCCC2.3* are orthologs of the *Saccharomyces cerevisiae CCC2*, which encodes a Cu-ATPase transporting Cu to Cu containing proteins in the trans-Golgi region (Yuan *et al*., 1995). *RiCRD1* is ortholog of *CaCRD1* of the pathogenic yeast *Candida albicans*, which encodes a P_{1B}-ATPase that exports excess Cu out of the cell, providing Cu resistance (Riggle and Kumamoto, 2000; Weissman *et al*., 2000).

The aim of this work was to characterize the *R. irregularis RiCRD1* gene to better understand the mechanisms of metal homeostasis in AM fungi. Our data suggest that the *RiCRD1* gene product plays a role in *R. irregularis* metal tolerance by detoxifying metal excess out of the fungus as well as in symbiotic Cu transport by releasing Cu from the arbuscules to the apoplast of the symbiotic interface. Our gene expression data also indicate that *R. irregularis* mainly uses a metal efflux based-strategy to cope with Cu toxicity.

2. **Materials and methods**

2.1. Biological materials and growth conditions

Rhizophagus irregularis (Blaszk., Wubet, Renker & Buscot) C. Walker & A. Schüßler DAOM 197198 monoxenic cultures were established on Ri T-DNA transformed carrot (*Daucus carota* L. clone DC2) roots in two-compartment Petri dishes filled with solid M medium (Chabot *et al*., 1992), according to St-Arnaud *et al.* (1996) with some modifications. Briefly, cultures were started in one compartment of the Petri dish by placing some non-mycorrhizal carrot root fragments together with a

125 fungal inoculum containing ERM, mycorrhizal roots and spores. Plates were incubated
126 in the dark at 24°C for 6-8 weeks until the other compartment was densely colonized by
127 the fungus and roots. The oldest compartment was removed and filled with liquid M
128 medium without sucrose (M-C medium) and the fungal mycelium was allowed to
129 colonize this compartment (hyphal compartment) during the two subsequent weeks
130 (Control plates) (Fig. 1).

131 For the Cu deficiency treatment, monoxenic cultures were started with roots and
132 an AM fungal inoculum previously grown in M media without Cu and established in M
133 media without Cu. For treatments with high Cu or Cd concentrations, the M-C medium
134 of the hyphal compartment was removed and replaced with fresh liquid M-C medium
135 (Control, 0.5 µM $CuSO_4$) or with M-C medium supplemented with 250 µM $CuSO_4$, 500
136 µM $CuSO_4$ or 45 µM $CdSO_4$. The time of medium exchange was referred as time 0.
137 Mycelia were collected 1, 2 and 7 days after Cu addition and 1, 3, 6, 12, 24 and 48
138 hours after Cd supplementation. ERM of all treatments was frozen in liquid N and
139 stored at - 80°C until used.

140 For gene expression comparison between ERM and IRM (intraradical
141 mycelium), several non-mycorrhizal carrot roots pieces were placed on the top of a
142 densely fungal colonized compartment and grown for 15 days at 24°C. Roots were
143 carefully collected with tweezers under a binocular microscope trying to remove the
144 attached extraradical hyphae, and frozen in liquid N and stored at - 80°C until used. An
145 aliquot of root fragments was separated to estimate mycorrhizal colonization.

146 *R. irregularis* ERM was also collected from mycorrhizal plants grown in the *in*
147 *vivo* whole plant bidimensional experimental system described by Pepe *et al.* (2017)
148 with some modifications. Briefly, chicory (*Cichorium intybus* L.) seeds were surface-
149 sterilized and germinated for 10-15 days in sterilized sand. Seedlings were transplanted

into 50 mL pots filled with sterilized sand and inoculated with an inoculum obtained from monoxenic cultures. Pots were placed in sun-transparent bags (Sigma-Aldrich, B7026) and maintained during one month in a growth chamber at 24 / 21°C day/night and 16 h light photoperiod. The root system of each plant was cleaned, wrapped in a nylon net (41 µM mesh, Millipore NY4100010) and placed between two 13 cm diameter membranes of mixed cellulose esters (0.45 µm pore diameter size, MF-Millipore HAWP14250) in 14 cm diameter Petri dishes having a hole on the edge to allow plant shoot growth and containing sterilized sand (Fig. 1). Petri plates containing plants were sealed with parafilm, wrapped with aluminum foil, placed into sun-transparent bags and maintained in a growth chamber. Plants were watered weekly with a 0.5× modified Hoagland nutrient solution containing 125 µM KH_2PO_4 and 0.16 µM $CuSO_4$ (control treatment) or without Cu (Cu deficiency treatment). Petri dishes were opened 2 weeks after preparing the root sandwiches, and ERM spreading from the nylon net onto the membranes was collected with tweezers, frozen in liquid N and stored at - 80°C until used. Roots wrapped in the nylon net were also frozen and stored at - 80°C. An aliquot of the roots was separated to estimate mycorrhizal colonization.

Tomato (*Solanum lycopersicum* L., cv. Moneymaker) mycorrhizal roots were collected from plants grown in pot cultures. Briefly, germinated seeds were transferred to 1.5 L pots containing a sterile mixture of sand:vermiculite (1:1, v/v) supplemented (10 %) with a substrate-based inoculum of *R.irregularis*. Plants were grown in a controlled environmental chamber with 65-75% relative humidity, day/ night temperatures of 25/ 18°C, and a photoperiod of 16 h at 350 µmol photons m^{-2} s^{-1}. Roots were harvested 8 weeks after inoculation.

The *Saccharomyces cerevisiae* strains used in this study were the mutants DTY113 (*cup1Δ*) and WYT (*yap1Δ*), lacking the metallothionein CUP1 and the

transcription factor yap1, respectively (Tamai *et al.*, 1993; Kuge and Jones, 1994). Detailed characteristics of yeast strains are listed in Table S1. Yeast cells were maintained on YPD or minimal synthetic dextrose (SD) medium, supplemented with the appropriate amino acids.

2.2. Mycorrhizal colonization

Mycorrhizal colonization was assessed after trypan blue staining (Phillips and Hayman, 1970) according to the Trouvelot method (Trouvelot *et al.* 1986). The abundance of AM fungus in the roots was also determined molecularly by determining the expression levels of the *R. irregularis* elongation factor 1α (*RiEF1α*; GenBank Accession No. DQ282611), using as internal control the elongation factor 1α of the corresponding host plant (*D. carota DcEF1α*, GenBank Accession No. XM_017391845; *C. intybus CiEF1α*, GenBank Accession No. KP752079).

2.3. RNA isolation and cDNA synthesis

The Plant RNeasy Kit (Qiagen) was used to extract total RNA from the ERM and mycorrhizal carrot roots developed in monoxenic cultures following manufacturer's instructions. Total RNA from mycorrhizal chicory roots was extracted using the phenol/SDS method followed by LiCl precipitation as described by Kay *et al.* (1987). The isolated RNAs were DNase treated with the RNA-free DNase set (Qiagen) according to manufacturer's instructions and quantified with the Nanodrop 1000 Spectrophotometer (Thermo Scientific). 1 µg of each RNA was used for the cDNA synthesis in a 20 µL final volume reaction containing 200 U of SuperScript III Reverse Transcriptase (Invitrogen) and 2.5 µM oligo (dT) 20 primer (Invitrogen), following the manufacturer's instructions.

199 *2.4. Gene isolation*

200 The *RiCRD1* gene sequence was previously identified by Tamayo *et al*. (2014) in
201 the *R. irregularis* genome available in the JGI website
202 (https://genome.jgi.doe.gov/portal/). The 5′ and 3′ ends were experimentally confirmed
203 by rapid amplification of cDNA ends (RACE) using the SMARTer® RACE 5′/3′ kit
204 (Clontech) and the *RiCRD1*-specific primers listed in Table S2. Genomic clone and full-
205 length cDNA of *RiCRD1* were obtained by PCR amplification of *R. irregularis* genomic
206 DNA and cDNA, respectively, from ERM grown under control conditions in
207 monoxenic cultures, using a set of primers flanking the complete open reading frame
208 (Table S2). PCR products were cloned into pENTR/D-TOPO (Invitrogen) via TOPO
209 reaction. The full-length cDNA was then cloned into the yeast expression vector
210 pDRf1-GW (Addgene) by using the Gateway LR Clonase recombination system
211 (Invitrogen).

212 *2.5. Sequence Analysis*

213 Transmembrane domains of the protein were predicted using the TMHMM Server
214 v.2.0 (http://www.cbs.dtu.dk/services/TMHMM/). The E1-E2 ATPase, hydrolase and
215 heavy metal associated domains were identified via the Pfam Software v. 32.0
216 (https://pfam.xfam.org/). Additionally, CD-Search
217 (https://www.ncbi.nlm.nih.gov/Structure/cdd/wrpsb.cgi) was used to verify the presence
218 of the P-type ATPase Cu-like signature cd02094 (NCBI). These results were used to
219 generate a structural model of RiCRD1 using MyDomains tool of Prosite
220 (https://prosite.expasy.org/mydomains/). Protein subcellular localization was predicted
221 by WoLF PSORT (https://wolfpsort.hgc.jp/).

222 Additionally, RiCRD1 full sequence was used as a query to identify orthologs
223 through Blastp searches in other Glomeromycotina species deposited on the JGI

(*Rhizophagus clarus* HR1, Kobayashi *et al.*, 2018; *Gigaspora rosea* v1.0, *Rhizophagus cerebriforme* DAOM 227022 v1.0, *Rhizophagus diaphanus* v1.0, Morin *et al.*, 2019; *Gigaspora margarita* BEG34, Venice *et al.*, 2020; *Geosiphon pyriformis*, Malar *et al.*, 2021) and NCBI websites. These sequences were aligned using Muscle v3.7 software with the complete HMA family of *R. irregularis*, other HMA-like fungal proteins from representatives of different taxonomic groups and the HMA proteins from the model plants *Arabidopsis thaliana* and *Oryza sativa*. Alignments were imported to the IQ-TREE software v1.6.12 (Nguyen *et al*., 2015) with parameters -nt AUTO, -bb 1000 -m TESTMERGE. The maximum likelihood tree was constructed following the model of evolution LG+I+G4 (best-fit model according to ModelFinder; Kalyaanamoorthy *et al*., 2017). Finally, the phylogenetic tree was plotted using the Interactive Tree of Life (iTOL) suite software v4 (Letunic and Bork, 2016).

2.6. Functional complementation analyses in yeast

Metal hypersensitive yeast mutants *cup1Δ* and *yap1Δ* were transformed with the resulting *RiCRD1* construct or with the corresponding empty vector (negative control) using a lithium acetate-based method (Gietz and Schiestl, 2007). Transformants were selected in SD medium by autotrophy to uracil. For drop tests, transformants were grown to exponential phase in SD medium without uracil. Cells were harvested by centrifugation, washed twice and adjusted to a final OD_{600} of 1. Then, 5 µL of serial 1:10 dilutions were spotted on the corresponding selective medium. The transformed *cup1Δ* cells were spotted onto SD medium without uracil supplemented or not with 75µM $CuSO_4$ or with 100 µM $CdSO_4$ and *yap1Δ* cells onto SD medium without uracil supplemented or not with 2 mM $CuSO_4$ or with 100 µM $CdSO_4$. Plates were incubated 5 days at 30 ºC.

2.7. Real-time quantitative RT-PCR

Gene expression patterns were analyzed in an iQ™5 Multicolor Real-Time PCR Detection System (Bio-Rad) using iQ™ SYBR Green Supermix (Bio-Rad) and the specific primers listed in Table S2. The program consisted in an initial incubation at 95°C for 3 min, followed by 38 cycles of 95°C for 30 s, 58°C for 30 s and 72°C for 30 s, at the end of which the fluorescence signal was measured. The specificity of the PCR amplification procedure was checked with a heat-dissociation protocol (from 58 to 95°C) after the final PCR cycle. Efficiency of the different primer sets was in the range 95-105 %. Since RNA extracted from mycorrhizal roots contains plant and fungal RNAs, specificity of the primer pairs was also analyzed by PCR amplification of carrot and chicory cDNA from non-mycorrhizal carrot and chicory roots. The relative abundance of the transcripts was calculated using $2^{-\Delta\Delta CT}$ method (Livak and Schmittgen, 2001) and normalized with the *R. irregularis* elongation factor 1α (*RiEF1α*; GenBank Accession No. DQ282611; Benabdellah *et al*., 2009). All determinations were performed in at least three biological samples with the threshold cycle (Ct) determined in duplicate in at least two independent PCRs.

2.8. In situ *hybridization of* RiCRD1 *transcripts in mycorrhizal roots*

200 bp sense and antisense probes of RiCRD1 and 18S RNA were generated by two nested PCR reactions using gene-specific primers containing a 5´overhang to allow their fusion to the T7 RNA polymerase promoter sequence (Table S2). The first PCR was carried out on cDNA from ERM grown under control conditions in monoxenic cultures with the primer pairs RiCRD1-T7-Pup and RiCRD1-Pdown or RiCRD1-Pup and RiCRD1-T7-Pdown. The second PCR was performed using 1 µL of a 1/100 dilution of the amplicon and the primer pairs E-T7 and RiCRD1-Pdown or RiCRD1-Pup and E-T7. Both amplifications were performed with GoTaq®G2 DNA polymerase (Promega) in a

final volume reaction of 25 µL, using the protocol: 94°C for 3 min, followed by 40 cycles of 94°C for 30 s, 56°C for 30 s and 72°C for 30 s. Amplification products were purified by ethanol precipitation and used to obtain digoxigenin-UTP-labelled RNA probes using the MAXIscript® T7 Transcription Kit following manufacturer´s instructions (Invitrogen). 18S sense and antisense ribosome probes were used as a positive control (Garcia et *al.*, 2013).

Hybridization and detection of the probes were performed on 8 µm-thick sections of 8-week-old mycorrhizal tomato roots, as described in Jabnoune *et al.* (2009). Briefly, 3 mm root fragments were vacuum infiltrated in 4% (w/v) paraformaldehyde, 0.1% Triton X-100 in phosphate-buffered saline (10mM PBS), fixed overnight at 4°C and embedded in paraffin (ParaplastPlus, Leica BioSystems). Longitudinal and cross-sections of 8 µm-thickness were obtained using a microtome Leica RM2255 and mounted on silanized slides (Euromedex). Sections were deparaffinized with Safesolv (Labonord), rehydrated and treated at 37°C for 40 min with proteinase K (0.1 U mL^{-1}). To stop proteinase K activity, sections were washed twice for 5 min in an arrest buffer (20 mM Tris-HCl pH 7.5, 2 mM $CaCl_2$, 50 mM $MgCl_2$), once for 2 min in PBS containing 0.2% glycine and twice in PBS. Hybridizations were carried out in a humid chamber at 45°C for 15 h on dehydrated sections using 600 ng of the corresponding probe by slide, as described in Jabnoune *et al.* (2009) including the stringency washes. Non-linked probes were removed with 20 µg mL^{-1} RNase A for 30 min at 37°C. Immunological detection of digoxigenin-labelled RNA hybrids was performed with anti-digoxigenin antibodies conjugated with alkaline phosphatase enzyme (Roche), following manufacturer´s instructions. Finally, detection of hybridization signal was performed using Vector Blue Alkaline Phosphatase Substrate kit (Vector Laboratories) according manufacturer´s instructions and images were taken on the Nikon Eclipse Ni-E

299 microscope (Nikon Corporation, Tokyo, Japan), objectives Plan APO 20x NA 0.75, 40x
300 NA 0.95 and 100x NA 1.45. An aliquot of the same root fragments was separated to
301 estimate mycorrhizal colonization.

302 *2.9. Statistical Analyses*

303 Statistical analyses were performed with IBM SPSS Statistic software v.25. Data
304 were subjected to the Student´s t-test when two means were compared, or by one-way
305 ANOVA using post hoc comparison with Tukey´s b-test to detect differences among
306 groups of means. Results were accepted as significant at $P < 0.05$. The data are
307 expressed as mean +/- standard error. All the analyses are based on at least 3 biological
308 replicates per each treatment ($n \geq 3$).

309 *2.10. Gene Accession Numbers*

310 GeneBank Accession numbers of the *R. irregularis* gene analyzed in this study:
311 *RiCRD1* (XM_025327727), *RiMT1*, formerly named *GintMT1* (XM_025308927),
312 *RiABC1*, formerly named *GintABC1* (GQ249346), *RiPCS* (XM_025316197); RiMST2
313 (HM143864).

314

315 3. **Results**

316 *3.1. Sequence analyses of the* Rhizophagus irregularis *RiCRD1 heavy metal ATPase*

317 The full-length cDNA sequence of *RiCRD1* encodes a protein of 946 amino acids
318 (GenBank Accession No. XP_025169806). Comparison of the full-length cDNA with
319 the genomic sequence revealed the presence of two introns of 92 and 76 bp flanked by
320 the characteristic splicing sequences GT and AG at the 5' and 3' ends, respectively (Fig.
321 2). The RiCRD1 protein contains all the characteristic features of P_{1B}-type (CPx-type)
322 ATPases, including the conserved transmembrane cysteine-proline-cysteine motif

(CPC) that is essential for metal translocation. The protein contains eight transmembrane helices with the $CPCX_6P$ motif in the sixth transmembrane helix typical of the P_{1B-1} subgroup of metal ATPases that transport Cu^+ ions, two heavy metal associated domains (PF00403) in the N-terminus, the E1-E2 ATPase domain (PF00122), the hydrolase domain (PF00702) including the DKTGT phosphorylation signature sequence, and the invariant histidine-proline HP dipeptide at 41 residues C-terminal from the phosphorylation signature (Arguello, 2003; Arguello *et al*., 2007; Smith *et al*., 2014; Solioz and Vulpe, 1996). The presence of the complete signature (cd02094) characteristic of P-type ATPase Cu-like proteins was identified in the RiCRD1 sequence, including the two cysteine residues CXC in the sixth transmembrane helix; one tyrosine, one asparagine, and one proline YNX_4P residue in the seventh transmembrane helix and one methionine followed by serine residues MXXSS in the eighth transmembrane helix (Arguello, 2003) (Fig. 2). RiCRD1 was predicted to be located at the plasma membrane, with the N- and C-termini facing the cytoplasmic side, suggesting that RiCRD1 encodes a heavy metal ATPase that pumps excess Cu^+ out of the cytosol.

The phylogenetic analysis revealed that all fungal ATPases were clustered into two different groups separated from those of plants: a CCC2–like group clustering orthologs of the *S. cerevisiae* CCC2 Cu-ATPase (Yuan *et al*., 1995) and a group of fungal ATPases related to metal tolerance, which comprises two subgroups, the PCA1-like and CRD1-like ATPases. The PCA1-like subgroup clusters orthologs of a Cd-efflux plasma membrane ATPase of *S. cerevisiae* (Adle *et al.*, 2007) and the CRD1-like subgroup includes orthologs of the *C. albicans* plasma membrane ATPase that exports excess of Cu out of the cell (Yuan *et al*., 1995). RiCRD1 is placed in the CRD1-like clade, which suggests that it acts as a plasma membrane Cu efflux transporter. Blastp searches for

RiCRD1 homologues in the genomes of various Glomeromycotina species revealed that the *R. irregularis* genome, as well as the genome of most Glomeromycotina species, harbors one *CRD1*-like gene. However, two and three paralogues were identified in the genomes of *Funneliformis caledonium* and *Claroideoglomus candidum*, respectively. All Glomeromycotina CRD1 sequences were grouped together in the CRD1-like subgroup (Fig. 3). Except for the two CRD1 sequences of *Dentiscutata erythropus*, which have three heavy metal associated domains (PF00403), the Glomeromycotina sequences have two (Table S3).

3.2. RiCRD1 *encodes a functional protein involved in Cu tolerance*

Due to the difficulty of gene manipulation in AM fungi, functionality of RiCRD1 was evaluated by a complementation assay in yeast. Since *S. cerevisiae* lacks CRD1 orthologs, functional analysis of RiCRD1 was carried out by testing the ability of the full-length *RiCRD1* gene product to rescue metal sensitivity of the *cup1Δ* and *yap1Δ* mutant strains of *S. cerevisiae*. CUP1 is a metallothionein that confers heavy metal tolerance to yeast cells by sequestering metal ions in the cytosol via the thiol groups of its cysteine residues (Ecker et *al.*, 1986; Hamer, 1986) and the transcription factor yap1 controls various genes involved in heavy metal and oxidative stress tolerance in yeast (Kuge and Jones, 1994; Shine *et al.* 2015). Inactivation of yap-1 protein results in an oxidative stress sensitive phenotype (Toone and Jones, 1999). The *cup1Δ* and *yap1Δ* mutants are particularly sensitive to Cu and Cd and are, thus, suitable to highlight tolerant phenotypes induced by exogenous cDNAs (Wu *et al.*, 1993). Copper hypersensitivity of *cup1Δ* cells is due to their inability to sequester metal excess in the cytosol, while Cu hypersensitivity of the *yap1Δ* mutant results from the oxidative stress caused by the accumulation of free Cu in the cytosol. As shown in Fig. 4, *RiCRD1*-expressing cells enhanced Cu tolerance of *cup1Δ* and *yap1Δ* strains when gown in

media containing 75 µM and 2 mM of $CuSO_4$, respectively. These data indicate that *RiCRD1* encodes a functional protein that confers Cu tolerance to yeast cells.

Since the CaCRD1 ortholog of *C. albicans* has also been shown to be involved in resistance to Cd ion toxicity (Riggle and Kumamoto, 2000), we also tested whether RiCRD1 could additionally confer some kind of Cd protection to these mutant strains. However, either empty vector-transformed cells or those expressing *RiCRD1* were unable to grow in SD medium supplemented with a gradient of $CdSO_4$ concentrations up to 100 µM (data not shown).

3.3. RiCRD1 *expression is up-regulated in response to high concentration of Cu and Cd in the medium*

To investigate whether RiCRD1 could play a role in metal tolerance by detoxifying Cu excess out of the fungus, *RiCRD1* gene expression was assessed by real time quantitative RT-PCR (RT-qPCR) in ERM grown in monoxenic cultures under different Cu (250 and 500 µM) levels. As previously observed by Cornejo *et al*. (2013), some blue spores indicative of Cu compartmentalization were observed in ERM 2 days after Cu addition to the medium (Fig. 5A). Exposure of the mycelia to high Cu levels increased transcription of *RiCRD1* at all the time points analyzed (Fig. 5A). This increase in transcript accumulation reaches 25-30 times the control level in response to increasing Cu concentration in the medium and time. These results are consistent with a role of *RiCRD1* in Cu detoxification.

RiCRD1 transcript levels were also determined in monoxenically grown ERM exposed to 45 µM $CdSO_4$ for different time periods. Interestingly, in contrast to elevated Cu levels, *RiCRD1* expression was only transiently induced by Cd. A 3-fold induction was observed 3 and 6 h after Cd addition, followed by a significantly decrease in gene expression (Fig. 5B).

3.4. RiCRD1 is a major player in R. irregularis *Cu tolerance*

To get some clues about the significance of RiCRD1 on metal tolerance in *R. irregularis*, the *RiCRD1* transcript accumulations in Cu- and Cd- treated ERM were compared with the transcript accumulations of other Cu- and Cd-responsive genes previously identified in the *R. irregulars* genome*:* the metallothionein *RiMT1*, (González-Guerrero *et al*., 2007), the ABC-transporter *RiABC1* (González-Guerrero *et al.*, 2010), and the phytochelatin synthase *RiPCS* (Shine *et al.*, 2015). Transcript levels of *RiMT1* were not significantly affected by Cu, except in ERM exposed for 2 d to 500 µM $CuSO_4$ (Fig. 6A). In contrast, ERM exposure to 45 µM Cd resulted in a stable 2- to 5-fold down-regulation of *RiMT1* 12 to 48 h after the application of the treatment (Fig. 6B). *RiABC1* transcript levels were only significantly changed 2 and 7 days after ERM exposure to 500 µM $CuSO_4$ (2-fold increase) and 6 h after ERM exposure to 45 µM Cd (transient 5-fold increase) (Figs. 6C, D). Interestingly, *RiPCS* transcript accumulation was 2-fold reduced in response to Cu exposure but unchanged in response to Cd exposure (Figs. 6E, F). Therefore, the expression of *RiCRD1* was much more impacted in response to Cu than other metal regulators of the intracellular metal levels.

3.5. RiCRD1 *is more highly expressed in the intraradical mycelium*

To further understand the role that RiCRD1 could play in *R. irregularis* and in the symbiosis, we assessed its expression level in the ERM and IRM grown under optimal conditions in two experimental systems: monoxenic cultures and the *in vivo* whole plant bidimensional experimental system (sandwich system). Transcript levels of the *R. irregularis* high-affinity monosaccharide transporter *RiMST2,* which is strongly up-regulated in the IRM during AM symbiosis (Helber *et al*., 2011), was also determined as a marker of fungal activity. Carrot roots collected from the monoxenic cultures presented 10% of mycorrhizal colonization while the percentage of mycorrhizal

423 colonization of the chicory roots used to grow the fungus in the sandwich system was
424 78%. In both experimental systems, *RiMST2* and *RiCRD1* were more highly expressed
425 in the IRM than in the ERM. *RiCRD1* transcript levels were 18-fold higher in carrot
426 mycorrhizal roots than in ERM collected from monoxenic cultures and 25-fold higher in
427 mycorrhizal chicory roots than in ERM collected from the *in vivo* sandwich system
428 (Fig. 7). This expression pattern hints at the importance of RiCRD1 in the intraradical
429 phase of the fungus, where it might mediate the efflux of Cu from the fungus to the
430 apoplast of the symbiotic interface.

431 *3.6.* RiCRD1 *is expressed in the arbuscules*

432 Given that arbuscules developed in plant cortical cells are the main structures where
433 nutrient exchanges between symbionts take place, Cu transfer from the fungus to the
434 plant should occur in the arbuscule-colonized cortical cells (Luginbuehl and Oldroyd,
435 2017; MacLean *et al*., 2017). However, since the fungus develops other intraradical
436 structures, we decided to determine the specific fungal structure where *RiCRD1* is
437 expressed by performing an *in situ* hybridization assay in tomato roots presenting a 40%
438 of mycorrhizal colonization (Figs. 8A-B). As a positive control of hybridization and
439 RNA quality, expression of the 18S ribosomal gene was monitored (Fig. S1). *RiCRD1*
440 transcripts were clearly detected with the antisense probe in the arbuscules developed in
441 the inner cortical cells while no signal was detected in any other fungal structure. This
442 expression pattern indicates that arbuscules are likely the sites of Cu efflux (Figs. 8C-F).

443 *3.7. Expression of* RiCRD1 *decreases in conditions of Cu limitation mycorrhizae*
444 *generated in Cu-deprived media*

445 To test whether *RiCRD1* expression is affected by Cu availability, we assessed
446 the influence of growing the roots under Cu-limiting conditions on the transcription of

RiCRD1. For this purpose, transcript accumulation of *RiCRD1* was determined by RT-qPCR in *R. irregularis* colonized roots grown in monoxenic cultures and in the *in vivo* sandwich system in the presence (control) and absence of Cu (Cu deficiency). Cu deficiency decreased mycorrhizal colonization of the carrot and chicory roots developedin the monoxenic and *in vivo* cultures, respectively, in comparison to control conditions, which was confirmed molecularly by the quantification of the amount of the fungus within the root (Table S4). Accumulation of *RiCRD1* transcripts was lower in mycorrhizal roots grown in conditions of Cu limitation than in control conditions (0.5 μM Cu in monoxenic cultures and 0.16 μM in the *in vivo* sandwich system) (Fig. 9). These data suggest that Cu efflux from the fungus is reduced under Cu-limiting conditions.

4. **Discussion**

AM fungi play an important role in modulating plant Cu acquisition in a wide range of Cu concentrations. The potential of AM fungi to either increase plant Cu uptake in poor Cu soils or alleviate Cu toxicity has led to the hypothesis that AM function as a "buffer" to protect the plant against damage produced by lack or excess of Cu in the soil (Ferrol *et al*., 2016; Gómez-Gallego *et al*., 2019). Here, we report characterization of *RiCRD1*, a *R. irregularis* gene encoding a protein with a role in Cu tolerance, which, according to its sequence features, is most likely a plasma membrane Cu-ATPase.

4.1. Identification of RiCRD1 as a putative Cu-ATPase with a role in Cu tolerance

In silico analysis of the RiCRD1 protein and expression patterns of *RiCRD1* when the ERM was exposed to high Cu levels strongly suggest that RiCRD1 is the ortholog of the plasma membrane Cu efflux P_{1B1}-type ATPase CaCRD1 of *C. albicans*

(Riggle and Kumamoto, 2000; Weissman *et al*., 2000). RiCRD1 has all the characteristic features of P_{1B}-type ATPases, and more specifically of those belonging to the P_{1B-1} subgroup, including the complete cd2094 signature of Cu-like proteins that transport Cu^{+} ions and the invariant $CPCX_6P$ motif typical of the P_{1B-1} subgroup (Arguello, 2003). It contains eight transmembrane domains, with the CPC motif that is needed for metal translocation in the sixth transmembrane helix (Arguello *et al*., 2007). Additionally, the invariant HP dipeptide was found 40 residues downstream to the phosphorylation site. Although the function of this motif is still unknown, it seems to have some relevance since replacement of the histidine by a glutamic acid induces abnormalities of copper metabolism in the Wilson's disease (Bissig *et al*., 2001; Solioz and Vulpe, 1996; Tanzi *et al*., 1993). Interestingly, RiCRD1 has two heavy metal associated domains in the N-terminus, although only one strictly has the classical GMXCXXC motif. The first domain, GLTCASC, has the CXXC motif characteristic of proteins that bind copper (Camakaris *et al*., 1999; Migocka, 2015; Smith *et al*., 2014; Strausak *et al*., 1999), but the second methionine is changed by a leucine. The N-terminus of RiCRD1, as well as most of the Glomeromycotina CRD1-like sequences, presents a reduced number of metal binding domains in comparison with other eukaryote Cu-ATPases, which usually have multiple repeats of this domain (Arguello *et al*., 2007; Rensing *et al*., 1999). For instance, CaCRD1 has five metal binding domains, including two CXXC and three GMXCXXC motifs (Riggle and Kumamoto, 2000; Weissman *et al*., 2000). However, numerous prokaryotic Cu-transporting ATPases have a single N-terminal metal binding domain (Rensing *et al.*, 2000). A reduced number of CXXC N-terminal repeats seems to be a characteristic feature of Glomeromycotina CRD1 proteins. These N-terminal metal binding domains of P_{1B-1} subgroup are homologous to a number of metal chaperone proteins, can bind Cu^{+}, Cu^{2+}, Zn^{2+}, Cd^{2+}

and exchange metals with the related chaperons. A regulatory role rather than an essential catalytic role has been proposed for these N-terminus metal binding domains (Arguello, 2003).

Our yeast heterologous complementation assays show that *RiCRD1* encodes a protein with a role in Cu tolerance, as it was able to protect the metal hypersensitive yeast *cup1Δ* and *yap1Δ* mutants against Cu toxicity. Since Cu hypersensitivity of both yeast strains results from Cu overaccumulation in the cytosol, our complementation assays indicate that, at least in the heterologous system, RiCRD1 decreases Cu levels in the cytosol. Previously characterized P_{1B}-type ATPases from fungi and prokaryotes involved in Cu homeostasis exhibit tightly controlled transcriptional regulation consistent with their physiological roles (Arguello, 2003; Antsotegi-Uskola *et al.*, 2017; Antsotegi-Uskola *et al.*, 2020; Benes *et al.*, 2018; Wiemann *et al.* 2017). The strong up-regulation of *RiCRD1* in the ERM in response to high Cu concentration in the medium supports the notion that RiCRD1 can play a role in Cu detoxification in *R. irregularis* ERM. These observations, together with the structural features and predicted plasma membrane location of RiCRD1, strongly suggest a role for RiCRD1 in Cu efflux from the cytosol.

4.2. RiCRD1 and Cu tolerance in R. irregularis

RiCRD1 would enable the fungus to avoid the accumulation of intracellular toxic levels of Cu by facilitating Cu efflux through the plasma membrane. This hypothesis is supported by the low cytoplasmic concentrations of Cu detected in the *R. irregularis* ERM when exposed to high Cu levels (González-Guerrero et al., 2008). Our data showing that in the ERM subjected to the highest Cu concentrations *RiMT1* expression was just slightly and transiently induced, while *RiCRD1* was highly up-regulated suggests that *R. irregularis* uses the Cu efflux RiCRD1 pump as primary mechanism to

overcome Cu toxicity. Actually, the role of the *R. irregularis* metallothionein RiMT1 in Cu tolerance was attributed to its antioxidant activity against the metal-induced oxidative stress rather than on its metal chelation activity (González-Guerrero *et al*., 2007). These results are in agreement with those described in *C. albicans* and some filamentous fungi, such as *Aspergillus nidulans* (Antsotegi-Uskola *et al*., 2020; Riggle and Kumamoto, 2000; Weissman *et al*., 2000), but in contrast with what happens in *S. cerevisiae*, in which Cu resistance mainly relies on Cu chelation by the CUP1 metallothionein (Ecker *et al*., 1986; Thiele, 1988). Here, we propose for the first time that AM fungi use a Cu efflux strategy to cope with Cu toxicity. In addition to this Cu efflux strategy, as previously reported by Cornejo *et al*. (2013), *R. irregularis* compartmentalizes part of the excess Cu in some spores of the fungal colony, as some blue spores indicative of Cu accumulation were observed in some of the Cu-exposed ERM.

4.3. Cd tolerance in R. irregularis

In *C. albicans*, *CRD1* null mutants presented increased sensitivity not only to Cu but also to Cd ions (Riggle and Kumamoto, 2000). This raised the question of whether RiCRD1 could also have a secondary role in Cd resistance in *R. irregularis*. *RiCRD1* *e*xpression was up-regulated in the ERM exposed to Cd, although this induction was faster, transient and less intense than with Cu. However, failure of RiCRD1 to recover the phenotype of the yeast metal hypersensitive mutants *cup1Δ* and *yap1Δ* in media supplemented with Cd rules out a function for RiCRD1 in protection against Cd toxicity. These data suggest that RiCRD1 cannot transport Cd^{2+} ions, which is consistent with the fact that the P_{1B-1} subgroup of P_{1B}-ATPases are highly specific for the transport of monovalent Cu ions, the dominant intracellular species in eukaryotes (Nevitt *et al.*, 2012). Transient accumulation of *RiCRD1* transcripts during the early

546 stages of Cd exposure could be caused by disturbed metal homeostasis with transient
547 increase in cytosolic Cu. Alternatively, as previously stated by Antsotegi-Ukola *et al.*
548 (2017), some kind of interaction of CRD1-like proteins with Cd stress might take place
549 transiently when other more specific pathways for Cd detoxification are saturated.

550 Down-regulation of *RiMT1* expression by Cd indicates that Cd detoxification should
551 rely on other specific players and agrees with previous hypothesis that metallothioneins
552 do not constitute the primary control point for metal detoxification in *R. irregularis*
553 (González-Guerrero *et al*., 2007). Other candidate players of metal detoxification in *R.*
554 *irregularis* could be phytochelatins, small peptides synthetized enzymatically from
555 glutathione by phytochelatin synthase that form complexes with metals in the
556 cytoplasm, which are then transported into the vacuoles (Cobbett, 2000a; Heiss *et al*.,
557 2003; Mendoza-Cozatl *et al*., 2010). The *R. irregularis* genome encodes a phytochelatin
558 synthase (*RiPCS*) (Shine *et al*., 2015) that is not transcriptionally regulated by Cd.
559 Although PCSs were considered to be sparsely distributed in the fungal kingdom, a
560 recent analysis of the distribution of candidate PCS in fungal genomes reveals their
561 presence in many lineages (Shine *et al*., 2015). However, PCS are usually expressed
562 constitutively and activated post-translationally by various essential and non-essential
563 metals, being Cd the most effective (Bolchi *et al*., 2011; Pal and Rai, 2010). Despite the
564 regulatory mechanisms of PCS function remain elusive, it has been proposed that either
565 the metal alone or the GSH-metal complexes formed in the cytosol can interact with the
566 PCS cysteine residues (Cobbet, 2000b). Up-regulation by Cu and Cd of *RiABC1*, a gene
567 putatively encoding an ABC transporter that could be involved in metal transport into
568 the vacuoles (González-Guerrero *et al.*, 2010; Rekha *et al.*, 2021) suggests that long-
569 term acclimation to high levels of Cd would be achieved through metal accumulation
570 into the fungal vacuoles (González-Guerrero *et al.*, 2008; Park *et al.* 2012; Rekha *et al.*,

2021; Song *et al.*, 2014). However, further analyses are required to elucidate the role of RiCRD1 in the early response to Cd toxicity and to decipher the mechanisms of Cd tolerance in *R. irregularis*.

4.4. Nutritional and ecological relevance of RiCRD1

The finding that *RiCRD1* was strongly expressed in the intraradical fungal structures and more specifically in the arbuscules hints at the importance of this protein for the symbiosis. We propose that the putative Cu efflux pump RiCRD1 could be involved in Cu release from the arbuscules to the apoplast of the symbiotic interface. However, silencing of this gene by either host-induced gene silencing (HIGS) or virus-induced gene silencing (VIGS) is needed to confirm this hypothesis. Down-regulation of *RiCRD1* in the IRM by Cu deficiency suggests that under these conditions the fungus reduces Cu efflux out of the cytosol. In fact, the decrease in *RiCRD1* transcript accumulation in the IRM under Cu-limiting conditions could mean that the fungus restricts the transfer of Cu to the plant in order to satisfy its own demand. This hypothesis is supported by our previous observations that transcript levels of the plasma membrane Cu uptake transporter *RiCTR1* increase under Cu deficient conditions and that under these conditions the number of arbuscules is reduced (Gómez-Gallego *et al.*, 2019). Further physiological studies using radioactively labeled Cu and compartmented pot systems with separate soil zones for hyphal growth combined with molecular studies are required to understand the contribution and regulation of the mycorrhizal Cu uptake pathway under different Cu supplies. Blastp searches in Glomeromycotina species revealed at least one *CRD1*-like gene in all the examined species, suggesting that this Cu efflux mechanism must not be unique to *R. irregularis*, and it is probably shared by other AM fungi. Interestingly, *Funneliformis caledonium* displays two paralogs and *Claroideoglomus candidum* three. More than one *CRD1*-like gene copy

has been described in other fungi such as in *Aspergillus* spp. which, if functional, might provide some sort of adaptive advantage to their respective ecological niches as a result of increased Cu export efficiency (Yang et *al.*, 2018).

On the other hand, we have recently shown that AM increases expression of HMA genes putatively encoding proteins involved in Cu detoxification and balances mineral nutrient uptake improving nutritional status of maize plants grown in Cu contaminated soils (Gómez-Gallego *et al.*, 2022). Therefore, all these results together indicate that AM fungi are able not only to up-regulate their own intrinsic Cu detoxification mechanisms but also those of their host plants and highlight the importance of the HMA genes to achieve balanced Cu levels. A better understanding of Cu transport mechanisms by both partners could help to fine-tune their management in agricultural fields to achieve more sustainable systems including the development of metal alleviation strategies in metal contaminated soils.

5. **Conclusions**

In conclusion, data presented in this work show that the *R. irregularis* gene *RiCRD1* encodes a protein with a role in Cu tolerance, which most likely is a plasma membrane Cu-ATPase. This Cu^{+} exporting P-type ATPase could have a major impact not only on metal detoxification but also on Cu transport through the mycorrhizal pathway by releasing Cu into the apoplast of the symbiotic interface. Although this study represents a breakthrough in the understanding of Cu homeostasis in AM fungi, further studies are necessary to fully understand this complex Cu homeostatic network, which allows AM fungi to maintain Cu intracellular levels balanced in a wide range of environments.

Author contributions

Tamara Gómez-Gallego: Conceptualization, Methodology, Formal analysis, Investigation, Writing – original draft & editing. Mª Jesús Molina-Luzón: Methodology & Investigation. Genevieve Conéjéro: Methodology, Supervision, Writing – review & editing. Pierre Berthomieu: Methodology, Supervision, Writing – review & editing. Nuria Ferrol: Conceptualization, Methodology, Supervision, Funding acquisition, Project administration, Writing – original draft & editing.

Funding sources

This work was supported by grant PID2021-1255210B-I00 funded by MCIN/AEI/ 10.13039/501100011033 and by "ERDF A way of making Europe", by the "European Union".

Data statement

All gene sequences used in this study are available in GenBank or JGI databases as detailed, any further information can be provided by the corresponding author upon reasonable request.

Declaration of competing interest

The authors declare no conflict of interest.

Acknowledgments

We acknowledge the imaging facility MRI, member of the France-BioImaging national infrastructure supported by the French National Research Agency (ANR-10-INBS-04, «Investments for the future»), in Montpellier.

642 **Appendix A. Supplementary data**

643 Supplementary data to this article can be found online.

644 Table S1: *Saccharomyces cerevisiae* strains used in this work, Table S2: Primers used
645 in this study, Table S3: CRD1-like sequences identified in Glomeromycotina species,
646 Table S4: Effect of Cu limitation on mycorrhizal colonization, Fig. S1: Controls used in
647 the *in situ* hybridization experiment.

648

649 **References**

650 Adle, D.J., Sinani, D., Kim, H., Lee, J., 2007. A Cadmium-transporting P_{1B}-type
651 ATPase in yeast *Saccharomyces cerevisiae*. J. Biol. Chem. 282, 947–955.
652 https://doi.org/10.1074/jbc.M609535200

653 An, J., Zeng, T., Ji, C., de Graaf, S., Zheng, Z., Xiao, T.T., Deng, X., Xiao, S.,
654 Bisseling, T. Limpens, E., Pan, Z., 2019. A *Medicago truncatula* SWEET
655 transporter implicated in arbuscule maintenance during arbuscular mycorrhizal
656 symbiosis. New Phytol. 224, 396-408. https://doi.org/10.1111/nph.15975

657 Antsotegi-Uskola, M., Markina-Iñarrairaegui, A., Ugalde, U., 2017. Copper resistance
658 in *Aspergillus nidulans* relies on the P(I)-Type ATPase CrpA, regulated by the
659 transcription factor AceA. Front. Microbiol. 8, 912.
660 https://doi.org/10.3389/fmicb.2017.00912

661 Antsotegi-Uskola M., Markina-Iñarrairaegui A., Ugalde U., 2020. New insights into
662 copper homeostasis in filamentous fungi. Int. Microbiol. 23, 65-73.
663 https://doi.org/10.1007/s10123-019-00081-5

664 Arguello, J.M., Eren, E., Gonzalez-Guerrero, M., 2007. The structure and function of

heavy metal transport P1B-ATPases. BioMetals 20, 233–248. https://doi.org/10.1007/s10534-006-9055-6

Bååth, E., 1989. Effects of heavy metals in soil on microbial processes and populations (a review). Water Air Soil Pollut. 47, 335–379. https://doi.org/10.1007/bf00279331

Benabdellah, K., Azcón-Aguilar, C., Valderas, A., Speziga, D., Fitzpatrick, TB., Ferrol N., 2009. *GintPDX1* encodes a protein involved in vitamin B6 biosynthesis that is up-regulated by oxidative stress in the arbuscular mycorrhizal fungus *Glomus intraradices.* New Phytol. 184, 682-693. https://doi.org/10.1111/j.1469-8137.2009.02978.x

Benes, V., Leonhardt, T., Sacky, J., Kotrba, P., 2018. Two P1B-1-ATPases of *Amanita strobiliformis* with distinct properties in Cu/Ag transport. Front. Microbiol. 9, 747. https://doi.org/10.3389/fmicb.2018.00747

Bissig, K.D., Wunderli-Ye, H., Duda, P.W., Solioz, M., 2001. Structure-function analysis of purified *Enterococcus hirae* CopB copper ATPase: effect of Menkes/Wilson disease mutation homologues. Biochem. J. 357, 217–223. https://doi.org/10.1042/bj3570217

Bolchi, A., Ruotolo, R., Marchini, G., Vurro, E., di Toppi, L.S., Kohler, A., Tisserant, E., Martin, F., Ottonello, S., 2011. Genome-wide inventory of metal homeostasis-related gene products including a functional phytochelatin synthase in the hypogeous mycorrhizal fungus *Tuber melanosporum*. Fungal Genet. Biol. 48, 573–584. https://doi.org/10.1016/j.fgb.2010.11.003

Brands, M., Dörmann, P., 2022. Two AMP-binding domain proteins from *Rhizophagus irregularis i*nvolved in import of exogenous fatty acids. Mol. Plant Microbe. Interact. 35, 464-476. https://doi.org/10.1094/MPMI-01-22-0026-R

689 Brundrett, M.C., Tedersoo, L., 2018. Evolutionary history of mycorrhizal symbioses
690 and global host plant diversity. New Phytol. 220, 1108–1115.
691 https://doi.org/10.1111/nph.14976

692 Camakaris, J., Voskoboinik, I., Mercer, J.F., 1999. Molecular mechanisms of copper
693 homeostasis. Biochem. Biophys. Res. Commun. 261, 225–232.
694 https://doi.org/10.1006/bbrc.1999.1073

695 Chabot, S., Bécard, G., Piché, Y., 1992. Life cycle of *Glomus intraradix* in root organ
696 culture. Mycologia 84, 315–321. https://doi.org/10.2307/3760183

697 Chen, E. C. H, Morin, E., Beaudet, D., Noel, J., Yildirir, G., Ndikumana, S., *et al.* 2018.
698 High intraspecific genome diversity in the model arbuscular mycorrhizal symbiont
699 *Rhizophagus irregularis.* New Phytol. 220, 1161-1171.
700 https://doi.org//10.1111/nph.14989

701 Cobbett, C.S., 2000a. Phytochelatins and their roles in heavy metal detoxification. Plant
702 Physiol. 123, 825–832. https://doi.org/10.1104/pp.123.3.825

703 Cobbett, C.S., 2000b. Phytochelatin biosynthesis and function in heavy-metal
704 detoxification. Curr. Opin. Plant Biol. 3, 211-216. https://doi.org/10.1016/S1369-
705 5266(00)80067-9

706 Coccina, A., Cavagnaro, T.R., Pellegrino, E., Ercoli, L., McLaughlin, M.J., Watts-
707 Williams S.J., 2019. The mycorrhizal pathway of zinc uptake contributes to zinc
708 accumulation in barley and wheat grain. BMC Plant Biol. 19, 133.
709 https://doi.org/10.1186/s12870-019-1741-y

710 Cornejo, P., Pérez-Tienda, J., Meier, S., Valderas, A., Borie, F., Azcón-Aguilar, C.,
711 Ferrol, N., 2013. Copper compartmentalization in spores as a survival strategy of

712 arbuscular mycorrhizal fungi in Cu-polluted environments. Soil Biol. Biochem. 57,
713 925–928. https://doi.org/10.1016/j.soilbio.2012.10.031

714 Ecker, D.J., Butt, T.R., Sternberg, E.J., Neeper, M.P., Debouck, C., Gorman, J.A.,
715 Crooke, S.T., 1986. Yeast metallothionein function in metal ion detoxification. J.
716 Biol. Chem. 261, 16895–16900. https://doi.org/10.1016/S0021-9258(19)75973-0

717 Ezawa, T., Maruyama, H., Kikuchi, Y., Yokoyama, K., Masuta, C., 2020. Application
718 of virus-induced gene silencing to arbuscular mycorrhizal fungi, in: Ferrol, N.,
719 Lanfranco, L. (Eds.), Arbuscular mycorrhizal fungi: methods and protocols.
720 Methods Mole. Biol. 2146, 249-254

721 Ferrol, N., Azcón-Aguilar, C., Pérez-Tienda, J., 2019. Review: Arbuscular mycorrhizas
722 as key players in sustainable plant phosphorus acquisition: An overview on the
723 mechanisms involved. Plant Sci. 280, 441-447.
724 https://doi.org/10.1016/j.plantsci.2018.11.011

725 Ferrol, N., González-Guerrero, M., Valderas, A., Benabdellah, K., Azcón-Aguilar, C.,
726 2009. Survival strategies of arbuscular mycorrhizal fungi in Cu-polluted
727 environments. Phytochem. Rev. 8, 551–559. https://doi.org/10.1007/s11101-009-
728 9133-9

729 Ferrol, N., Tamayo, E., Vargas, P., 2016. The heavy metal paradox in arbuscular
730 mycorrhizas: from mechanisms to biotechnological applications. J. Exp. Bot. 67,
731 6253–6265. https://doi.org/10.1093/jxb/erw403

732 Festa, R.A., Thiele, D.J., 2011. Copper: an essential metal in biology. Curr. Biol. 21,
733 R877-R883. https://doi.org/10.1016/j.cub.2011.09.040.

734 Garcia K., Haider M.Z., Delteil A., Corratgé-Faillie C., Conéjero G., Tatry M., Becquer

735 A., Amenc L., Sentenac H., Plassard P., Zimmermann S., 2013. Promoter-
736 dependent expression of the fungal transporter HcPT1. 1 under Pi shortage and its
737 spatial localization in ectomycorrhiza. Fungal Genet. Biol. 58, 53-61.
738 https://doi.org/10.1016/j.fgb.2013.06.007

739 Gietz, R. D., and Schiestl, R. H., 2007. High-efficiency yeast transformation using the
740 LiAc/SS carrier DNA/PEG method. Nat. Protoc. 2, 31–34.
741 https://doi.org/10.1038/nprot.2007.13

742 Gómez-Gallego, T., Benabdellah, K., Merlos, M.A., Jiménez-Jiménez, A.M., Alcon, C.,
743 Berthomieu, P., Ferrol, N., 2019. The *Rhizophagus irregularis* genome encodes
744 two CTR copper transporters that mediate cu import into the cytosol and a CTR-
745 like protein likely involved in copper tolerance. Front. Plant Sci. 10. 604
746 https://doi.org/10.3389/fpls.2019.00604

747 Gómez-Gallego, T., Valderas, A., van Tuinen, D., Ferrol, N., 2022. Impact of
748 arbuscular mycorrhiza on maize P(1B)-ATPases gene expression and ionome in
749 copper-contaminated soils. Ecotoxicol Env. Saf. 234, 113390.
750 https://doi.org/10.1016/j.ecoenv.2022.113390

751 González-Guerrero, M., Benabdellah, K., Valderas, A., Azcón-Aguilar, C., Ferrol, N.,
752 2010. *GintABC1* encodes a putative ABC transporter of the MRP subfamily
753 induced by Cu, Cd, and oxidative stress in *Glomus intraradices*. Mycorrhiza 20,
754 137–146. https://doi.org/10.1007/s00572-009-0273-y

755 González-Guerrero, M., Cano, C., Azcón-Aguilar, C., Ferrol, N., 2007. *GintMT1*
756 encodes a functional metallothionein in *Glomus intraradices* that responds to
757 oxidative stress. Mycorrhiza 17, 327–335. https://doi.org/10.1007/s00572-007-
758 0108-7

González-Guerrero, M., Melville, L.H., Ferrol, N., Lott, J.N.A., Azcón-Aguilar, C., Peterson, R.L., 2008. Ultrastructural localization of heavy metals in the extraradical mycelium and spores of the arbuscular mycorrhizal fungus *Glomus intraradices*. Can. J. Microbiol. 54, 103–110. https://doi.org/10.1139/w07-119

Halliwell, B., Gutteridge, J.M., 1984. Oxygen toxicity, oxygen radicals, transition metals and disease. Biochem. J. 219, 1–14. https://doi.org/10.1042/bj2190001

Hamer, D.H., 1986. Metallothionein. Annu. Rev. Biochem. 55, 913-951. https://doi.org/10.1146/annurev.bi.55.070186.004405

Hartmann, M., Voß, S., Requena, N., 2020. Host-induced gene silencing of arbuscular mycorrhizal fungal genes via *Agrobacterium rhizogenes*-mediated root transformation in *Medicago truncatula*, in: Ferrol, N., Lanfranco, L. (Eds.), Arbuscular mycorrhizal fungi: methods and protocols. Methods Mole. Biol. 2146, 239–249

Heiss, S., Wachter, A., Bogs, J., Cobbett, C., Rausch, T., 2003. Phytochelatin synthase (PCS) protein is induced in *Brassica juncea* leaves after prolonged Cd exposure. J. Exp. Bot. 54, 1833–1839. https://doi.org/10.1093/jxb/erg205

Helber, N., Wippel, K., Sauer, N., Schaarschmidt, S., Hause, B., Requena, N., 2011. A versatile monosaccharide transporter that operates in the arbuscular mycorrhizal fungus *Glomus* sp is crucial for the symbiotic relationship with plants. Plant Cell 23, 3812–3823. https://doi.org/10.1105/tpc.111.089813

Hui, J., An, X., Li, Z., Neuhäuser, B., Ludewig, U., Wu, X., Schulze, W.X., Chen, F., Feng, G., Lambers, H., Zhang, F., Yuan, L., 2022. The mycorrhiza-specific ammonium transporter ZmAMT3;1 mediates mycorrhiza-dependent nitrogen uptake in maize roots. Plant Cell. 34, 4066-4087.

https://doi.org/10.1093/plcell/koac225

Jabnoune, M., Espeout, S., Mieulet, D., Fizames, C., Verdeil, J.L., Conejero, G., Rodriguez-Navarro, A., Sentenac, H., Guiderdoni, E., Abdelly, C., Very, A.A., 2009. Diversity in expression patterns and functional properties in the rice HKT transporter family. Plant Physiol. 150, 1955–1971. https://doi.org/10.1104/pp.109.138008

Jiang, Y., Wang, W., Xie, Q., Liu, N., Liu, L., Wang, D., Zhang, X., Yang, C., Chen, X., Tang, D., Wang, E., 2017. Plants transfer lipids to sustain colonization by mutualistic mycorrhizal and parasitic fungi. Science 356, 1172-1175. https://doi.org/ 10.1126/science.aam9970

Kalyaanamoorthy, S., Minh, B.Q., Wong, T.K.F., Von Haeseler, A., Jermiin, L.S., 2017. ModelFinder: Fast model selection for accurate phylogenetic estimates. Nat. Methods 14, 587-589. https://doi.org/10.1038/nmeth.4285

Kay, R., Chan, A., Daly, M., McPherson, J., 1987. Duplication of CaMV 35S promoter sequences creates a strong enhancer for plant genes. Science 236, 1299–1302. https://doi.org/10.1126/science.236.4806.1299

Kobayashi, Y., Maeda, T., Yamaguchi, K., Kameoka, H., Tanaka, S., Ezawa, T., Shigenobu, S., Kawaguchi, M., 2018. The genome of *Rhizophagus clarus* HR1 reveals a common genetic basis for auxotrophy among arbuscular mycorrhizal fungi. BMC Genomics 19, 465. https://doi.org/10.1186/s12864-018-4853-0

Kuge, S., and Jones, N., 1994. YAP1 dependent activation of *TRX2* is essential for the response of *Saccharomyces cerevisiae* to oxidative stress by hydroperoxides. EMBO J. 13, 655–664. https://doi.org/10.1002/j.1460-2075.1994.tb06304.x

Lanfranco, L., Fiorilli, V., Gutjahr, C., 2018. Partner communication and role of nutrients in the arbuscular mycorrhizal symbiosis. New Phytol. 220, 1031-1046. https://doi.org/10.1111/nph.15230

Lee, Y.-J., George, E., 2005. Contribution of mycorrhizal hyphae to the uptake of metal cations by cucumber plants at two levels of phosphorus supply. Plant Soil 278, 361–370. https://doi.org/10.1007/s11104-005-0373-1

Letunic, I., Bork, P., 2016. Interactive tree of life (iTOL) v3: an online tool for the display and annotation of phylogenetic and other trees. Nucleic Acids Res. 44, W242-245. https://doi.org/10.1093/NAR/GKW290

Li, X.-L., Marschner, H., George, E., 1991. Acquisition of phosphorus and copper by VA-mycorrhizal hyphae and root-to-shoot transport in white clover. Plant Soil 136, 49–57. https://doi.org/10.1007/bf02465219

Linder, M. C., 1991. Biochemistry of Copper, Plenum Press, New York

Livak, K.J., Schmittgen, T.D., 2001. Analysis of relative gene expression data using real-time quantitative PCR and the 2(-Delta Delta C(T)) Method. Methods 25, 402–408. https://doi.org/10.1006/meth.2001.1262

Luginbuehl, L.H., Oldroyd, G.E.D., 2017. Understanding the arbuscule at the heart of endomycorrhizal symbioses in plants. Curr. Biol. 27, R952-963. https://doi.org/10.1016/j.cub.2017.06.042

Ma Y., Ankit, Tiwari J., Bauddh K., 2022. Plant-mycorrhizal fungi interactions in phytoremediation of geogenic contaminated soils. Front. Microbiol. 13, 843415. https://doi.org/10.3389/fmicb.2022.843415.

MacLean, A.M., Bravo, A., Harrison, M.J., 2017. Plant signaling and metabolic

pathways enabling arbuscular mycorrhizal symbiosis. Plant Cell 29, 2319–2335. https://doi.org/10.1105/tpc.17.00555

Macomber, L., Imlay, J.A., 2009. The iron-sulfur clusters of dehydratases are primary intracellular targets of copper toxicity. Proc. Natl. Acad. Sci. U. S. A. 106, 8344–8349. https://doi.org/10.1073/pnas.0812808106

Malar C, M., Krüger, M., Krüger, C., Wang, Y., Stajich, J.E., Keller, J., Chen, E.C.H., Yildirir, G., Villeneuve-Laroche, M., Roux, C., Delaux, P.M., Corradi, N., 2021. The genome of *Geosiphon pyriformis* reveals ancestral traits linked to the emergence of the arbuscular mycorrhizal symbiosis. Curr. Biol. 31. 1570-1577. https://doi.org/10.1016/j.cub.2021.01.058

Mendoza-Cozatl, D.G., Zhai, Z., Jobe, T.O., Akmakjian, G.Z., Song, W.Y., Limbo, O., Russell, M.R., Kozlovskyy, V.I., Martinoia, E., Vatamaniuk, O.K., Russell, P., Schroeder, J.I., 2010. Tonoplast-localized Abc2 transporter mediates phytochelatin accumulation in vacuoles and confers cadmium tolerance. J. Biol. Chem. 285, 40416–40426. https://doi.org/10.1074/jbc.M110.155408

Migocka, M., 2015. Copper-transporting ATPases: The evolutionarily conserved machineries for balancing copper in living systems. IUBMB Life 67, 737–745. https://doi.org/10.1002/iub.1437

Moreno Jiménez, E., Ferrol, N., Corradi, N., Peñalosa, J.M., Rillig, M.C. 2023. The potential of arbuscular mycorrhizal fungi to enhance metallic micronutrient uptake and mitigate food contamination in agriculture: prospects and challenges. New Phytol. https://doi.org/10.1111/nph.19269

Morin, E., Miyauchi, S., San Clemente, H., Chen, E.C.H., Pelin, A., de la Providencia, I., Ndikumana, S., Beaudet, D., Hainaut, M., Drula, E., Kuo, A., Tang, N., Roy, S.,

Viala, J., Henrissat, B., Grigoriev, I. V, Corradi, N., Roux, C., Martin, F.M., 2019. Comparative genomics of *Rhizophagus irregularis*, *R. cerebriforme*, *R. diaphanus* and *Gigaspora rosea* highlights specific genetic features in Glomeromycotina. New Phytol. 222, 1584–1598. https://doi.org/10.1111/nph.15687

Nevitt, T., Ohrvik, H., Thiele, DJ., 2012. Charting the travels of copper in eukaryotes from yeast to mammals. Biochim. Biophys. 1823, 1580-1593. https://doi.org/10.1016/j.bbamcr.2012.02.011

Nguyen, L.T., Schmidt, H.A., Von Haeseler, A., Minh, B.Q., 2015. IQ-TREE: A fast and effective stochastic algorithm for estimating maximum-likelihood phylogenies. Mol. Biol. Evol. 32. 268-274. https://doi.org/10.1093/molbev/msu300

Pal, R., Rai, J.P.N., 2010. Phytochelatins: peptides involved in heavy metal detoxification. Appl. Biochem. Biotechnol. 160, 945–963. https://doi.org/10.1007/s12010-009-8565-4

Palmgren, M.G., Nissen, P., 2011. P-type ATPases. Annu. Rev. Biophys. 40, 243–266. https://doi.org/10.1146/annurev.biophys.093008.131331

Park, J., Song, WY., Ko, D., Eom, Y., Hansen, TH., Schiller, M., Lee, TG., Martinoia, E., Lee, Y., 2012. The phytochelatin transporters AtABCC1 and AtABCC2 mediate tolerance to cadmium and mercury. Plant J. 69, 278-288. https://doi.org/10.1111/j.1365-313X.2011.04789.x

Pepe, A., Sbrana, C., Ferrol, N., Giovannetti, M., 2017. An *in vivo* whole-plant experimental system for the analysis of gene expression in extraradical mycorrhizal mycelium. Mycorrhiza 27, 659–668. https://doi.org/10.1007/s00572-017-0779-7

Phillips, J.M., Hayman, D.S., 1970. Improved procedures for clearing roots and staining

parasitic and vesicular-arbuscular mycorrhizal fungi for rapid assessment of infection. Trans. Br. Mycol. Soc. 55, 158–161. https://doi.org/10.1016/S0007-1536(70)80110-3

Pozo, M.J., Zabalgogeazcoa, I., de Aldana, B.R.V., and Martinez-Medina, A., 2021. Untapping the potential of plant mycobiomes for applications in agriculture. Curr. Opin. Plant Biol. 60, 102034. https://doi.org/10.1016/j.pbi.2021.102034

Rekha, K., Balasundaram, U., Keeran, NS., 2021. 3 - Role of ABC transporters and other vacuolar transporters during heavy metal stress in plants, in: Roychoudhury, A., Tripathi, DK., Deshmukh, R. (Eds.), Metal and nutrient transporters in abiotic stress. Academic Press, 55-76

Rensing, C., Fan, B., Sharma, R., Mitra, B., Rosen, BP., 2000. CopA: An *Escherichia coli* Cu(I)-translocating P-type ATPase. Proc. Natl. Acad. Sci. U S A. 97, 652-656. https://doi.org/10.1073/pnas.97.2.652

Rensing, C., Ghosh, M., Rosen, B.P., 1999. Families of soft-metal-ion-transporting ATPases. J. Bacteriol. 181, 5891–5897. https://doi.org/10.1128/JB.181.19.5891-5897.1999

Riggle, P.J., Kumamoto, C.A., 2000. Role of a *Candida albicans* P1-type ATPase in resistance to copper and silver ion toxicity. J. Bacteriol. 182, 4899–4905. https://doi.org/10.1128/JB.182.17.4899-4905.2000

Roth, R., Paszkowski, U., 2017. Plant carbon nourishment of arbuscular mycorrhizal fungi. Curr. Opin. Plant Biol. 39, 50–56. https://doi.org/10.1016/j.pbi.2017.05.008

Ruytinx, J., Kafle, A., Usman, M., Coninx, L.,Zimmermann, García, K., 2020. Micronutrient transport in mycorrhizal symbiosis; zinc steals the show. Fungal

Biol. Rev. 34, 1-9. https://doi.org/10.1016/j.fbr.2019.09.001

Saitoh, Y., Izumitsu, K., Tanaka, C., 2009. Phylogenetic analysis of heavy-metal ATPases in fungi and characterization of the copper-transporting ATPase of *Cochliobolus heterostrophus*. Mycol. Res. 113, 737–745. https://doi.org/10.1016/j.mycres.2009.02.009

Salustros, N., Grønberg, C., Abeyrathna, N.S. *et al.* 2022. Structural basis of ion uptake in copper-transporting P1B-type ATPases. Nat. Commun. 13, 5121 https://doi.org/10.1038/s41467-022-32751-w

Senovilla, M., Abreu, I., Escudero, V., Cano, C., Bago, A., Imperial, J., González-Guerrero, M., 2020. MtCOPT2 is a Cu+ transporter specifically expressed in *Medicago truncatula* mycorrhizal roots. Mycorrhiza 30, 781–788. https://doi.org/10.1007/s00572-020-00987-3

Shi, J., Wang, X., Wang, E., 2023. Mycorrhizal symbiosis in plant growth and stress adaptation: from genes to ecosystems. Annu. Rev. Plant Biol. 74, 569-607. https://doi.org/10.1146/annurev-arplant-061722-090342

Shi, W., Zhang, Y., Chen, S., Polle, A., Rennenberg, H., Luo, Z-B., 2019. Physiological and molecular mechanisms of heavy metal accumulation in nonmycorrhizal versus mycorrhizal plants. Plant Cell Environ. 42, 1087– 1103. https://doi.org/10.1111/pce.13471

Shine, A.M., Shakya, V.P.S., Idnurm, A., 2015. Phytochelatin synthase is required for tolerating metal toxicity in a basidiomycete yeast and is a conserved factor involved in metal homeostasis in fungi. Fungal Biol. Biotechnol. 2, 3. https://doi.org/10.1186/s40694-015-0013-3

922 Smith, A.T., Smith, K.P., Rosenzweig, A.C., 2014. Diversity of the metal-transporting
923 P1B-type ATPases. J. Biol. Inorg. Chem. 19, 947–960.
924 https://doi.org/10.1007/s00775-014-1129-2

925 Solioz, M., Vulpe, C., 1996. CPx-type ATPases: a class of P-type ATPases that pump
926 heavy metals. Trends Biochem. Sci. 21, 237–241. https://doi.org/10.1016/S0968-
927 0004(96)20016-7

928 Spatafora, J.W., Chang, Y., Benny, G.L., Lazarus, K., Smith, M.E., Berbee, M.L.,
929 Bonito, G., Corradi, N., Grigoriev, I., Gryganskyi, A., James, T.Y., O'Donnell, K.,
930 Roberson, R.W., Taylor, T.N., Uehling, J., Vilgalys, R., White, M.M., Stajich, J.E.,
931 2016. A phylum-level phylogenetic classification of zygomycete fungi based on
932 genome-scale data. Mycologia 108, 1028-1046. https://doi.org/10.3852/16-042

933 St-Arnaud, M., Hamel, C., Vimard, B., Caron, M., Fortin, J.A., 1996. Enhanced hyphal
934 growth and spore production of the arbuscular mycorrhizal fungus *Glomus*
935 *intraradices* in an *in vitro* system in the absence of host roots. Mycol. Res. 100,
936 328–332. https://doi.org/10.1016/S0953-7562(96)80164-X

937 Song, WY., Mendoza-Cózatl, DG., Lee, Y., Schroeder, JI., Ahn, SN., Lee, HS., Wicker,
938 T., Martinoia, E., 2014. Phytochelatin-metal(loid) transport into vacuoles shows
939 different substrate preferences in barley and *Arabidopsis*. Plant Cell Environ. 37,
940 1192-1201. https://doi.org/10.1111/pce.12227

941 Strausak, D., Fontaine, S. La, Hill, J., Firth, S.D., Lockhart, P.J., Mercer, J.F.B., 1999.
942 The role of GMXCXXC metal binding sites in the copper-induced redistribution of
943 the Menkes protein. J. Biol. Chem. 274, 11170–11177.
944 https://doi.org/10.1074/jbc.274.16.11170

945 Tamayo, E., Gómez-Gallego, T., Azcón-Aguilar, C., Ferrol, N., 2014. Genome-wide

946 analysis of copper, iron and zinc transporters in the arbuscular mycorrhizal fungus
947 *Rhizophagus irregularis*. Front. Plant Sci. 5, 547.
948 https://doi.org/10.3389/fpls.2014.00547

949 Tamai, K.T., Gralla, E.B., Ellerby, L.M., Valentine, J.S., Thiele, D.J., 1993. Yeast and
950 mammalian metallothioneins functionally substitute for yeast copper-zinc
951 superoxide dismutase. Proc. Natl. Acad. Sci. USA 90, 8013-8017.
952 https://doi.org/10.1073/pnas.90.17.8013

953 Tanzi, R.E., Petrukhin, K., Chernov, I., Pellequer, J.L., Wasco, W., Ross, B., Romano,
954 D.M., Parano, E., Pavone, L., Brzustowicz, L.M., *et al*., 1993. The Wilson disease
955 gene is a copper transporting ATPase with homology to the Menkes disease gene.
956 Nat. Genet. 5, 344–350. https://doi.org/10.1038/ng1293-344

957 Thiele, D.J., 1988. ACE1 regulates expression of the *Saccharomyces cerevisiae*
958 metallothionein gene. Mol. Cell. Biol. 8, 2745–2752.
959 https://doi.org/10.1128/mcb.8.7.2745-2752.1988

960 Toone, W.M., Jones, N., 1999. AP-1 transcription factors in yeast. Curr. Opin. Genet.
961 Dev. 9, 55-61. https://doi.org/10.1016/s0959-437x(99)80008-2

962 Trouvelot, A., Kough, J.L., Gianinazzi-Pearson, V., 1986. Estimation of vesicular
963 arbuscular mycorrhizal infection levels. Research for methods having a functional
964 significance. Physiol. Genet. Asp. mycorrhizae = Asp. Physiol. Genet. des
965 mycorhizes Proc. 1st Eur. Symp. Mycorrhizae, Dijon, 1-5 July 1985.
966 https://doi.org/10.3/JQUERY-UI.JS

967 Venice, F., Ghignone, S., Salvioli di Fossalunga, A., Amselem, J., Novero, M., Xianan,
968 X., Sędzielewska Toro, K., Morin, E., Lipzen, A., Grigoriev, I. V., Henrissat, B.,

969 Martin, F.M., Bonfante, P., 2020. At the nexus of three kingdoms: the genome of
970 the mycorrhizal fungus *Gigaspora margarita* provides insights into plant,
971 endobacterial and fungal interactions. Environ. Microbiol. 22, 122-141.
972 https://doi.org/10.1111/1462-2920.14827

973 Wang, S., Chen, A., Xie, K., Yang, X., Luo, Z., Chen, J., Zeng, D., Ren, Y., Yang, C.,
974 Wang, L., Feng, H., López-Arredondo, D.L., Herrera-Estrella, L.R., Xu, G., 2020.
975 Functional analysis of the OsNPF4.5 nitrate transporter reveals a conserved
976 mycorrhizal pathway of nitrogen acquisition in plants. Proc. Natl. Acad. Sci. 117,
977 16649–16659. https://doi.org/10.1073/pnas.2000926117

978 Wang, S., Xie, X., Che, X., Lai, W., Ren, Y., Fan, X., Hu, W., Tang, M., Chen, H.,
979 2023. Host- and virus-induced gene silencing of HOG1-MAPK cascade genes in
980 Rhizophagus irregularis inhibit arbuscule development and reduce resistance of
981 plants to drought stress. Plant Biotechnol. J. 21, 866-883.
982 https://doi.org/10.1111/pbi.14006

983 Weissman, Z., Berdicevsky, I., Cavari, B.-Z., Kornitzer, D., 2000. The high copper
984 tolerance of *Candida albicans* is mediated by a P-type ATPase. Proc. Natl. Acad.
985 Sci. 97, 3520–3525. https://doi.org/10.1073/pnas.97.7.3520

986 Wiemann, P., Perevitsky, A., Lim, FY., Shadkchan, Y., Knox, BP., Landero Figueora,
987 JA., Choera, T., Niu, M., Steinberger, AJ., Wüthrich, M., Idol, RA., Klein, BS.,
988 Dinauer, MC., Huttenlocher, A., Osherov, N., Keller, NP., 2017. *Aspergillus*
989 *fumigatus* copper export machinery and reactive oxygen intermediate defense
990 counter host copper-mediated oxidative antimicrobial offense. Cell Rep. 19, 1008-
991 1021. https://doi.org/ 10.1016/j.celrep.2017.04.019

992 Wipf, D., Krajinski, F., Courty, P.-E., 2019. Trading on the arbuscular mycorrhiza

market: from arbuscules to common mycorrhizal networks. New Phytol. 223, 1127-1142. https://doi.org/10.1111/nph.15775

Wu, A., Wemmie, JA., Edgington, NP., Goebl, M., Guevara, JL., Moye-Rowley, WS., 1993. Yeast bZip proteins mediate pleiotropic drug and metal resistance. J. Biol. Chem. 268, 18850-18858

Xie, X., Lai, W., Che, X., Wang, S., Ren, Y., Hu, W., Chen, H., Tang, M., 2022. A SPX domain-containing phosphate transporter from *Rhizophagus irregularis* handles phosphate homeostasis at symbiotic interface of arbuscular mycorrhizas. New Phytol. 234, 650-671. https://doi.org/10.1111/nph.17973

Yang, K., Shadkchan, Y., Tannous, J., Landero Figueroa, J.A., Wiemann, P., Osherov, N., Wang, S., Keller, N.P., 2018. Contribution of ATPase copper transporters in animal but not plant virulence of the crossover pathogen *Aspergillus flavus*. Virulence. 9, 1273–1286. https://doi.org/10.1080/21505594.2018.1496774.

Yuan, D.S., Stearman, R., Dancis, A., Dunn, T., Beeler, T., Klausner, R.D., 1995. The Menkes/Wilson disease gene homologue in yeast provides copper to a ceruloplasmin-like oxidase required for iron uptake. Proc. Natl. Acad. Sci. U. S. A. 92, 2632–2636. https://doi.org/10.1073/pnas.92.7.2632

Figure captions

Fig. 1. Scheme of the two experimental systems used to grow *Rhizophagus irregularis*. (A) Monoxenic cultures established with transformed carrot roots (Ri T-DNA) in two-compartment Petri dishes containing M medium (St-Arnaud *et al.*, 1996) (*in vitro* culture system). (B) In vivo whole plant bidimensional experimental system established with chicory seedlings according to Pepe *et al.* (2017) with some modifications as detailed in Materials and Methods (sandwich system). CH: hyphal compartment; RC: root compartment; A: arbuscule; BAS: Branched Absorbing Structures; S: spores; ERM: extraradical mycelium; IRM: intraradical mycelium.

Fig. 2. Schematic representation of the structure of *R. irregularis* RiCRD1 depicting the position of characteristic features of P_{1B}-type ATPases. This model was generated with the MyDomains tool of Prosite (https://prosite.expasy.org/mydomains/) based on the results of the TMHMM Server v.2.0 (http://www.cbs.dtu.dk/services/TMHMM/) and the Pfam Software v. 32.0 (https://pfam.xfam.org/). Exon/intron organization of the *RiCRD1* genomic sequence, introns were illustrated with striped boxes and flanked by the canonical splicing sequences GT an AG at 5' and 3' ends, respectively.

Fig. 3. Phylogenetic relationships of HMA proteins. *R. irregularis* HMA proteins are in bold and GenBank accession numbers of all the protein sequences used for the analyses are provided. The maximum likelihood tree was constructed following the model of evolution LG+I+G4 for amino acid sequences in IQ-TREE software. Colors of the branches represent levels of significance obtained in the bootstrapping analyses to define each cluster, as indicated in the figure legend (1000 bootstrap replicates). Organisms: Ac, *Acaulospora colombiana*; Af, *Aspergillus fumigatus*; Afl, *Aspergillus flavus;* And, *Aspergillus nidulans;* An, *Aspergillus niger*; As, *Amanita strobiliformis*; At, *Arabidopsis thaliana*; Bc, *Botrytis cinerea*; Cc, *Coprinopsis cinerea*; Cp,

Cetraspora pellucida; Cg, *Colletotrichum gloeosporioides*; Clc, *Claroideoglomus candidum*; Cn, *Cryptococcus neoformans*; De, *Dentiscutata erythropus*; Dh, *Dentiscutata heterogama*; Deb, *Diversispora eburnea*; Dep, *Diversispora epigaea* Fc, *Funneliformis caledonium*; Gp, *Geosiphon pyriformis*; Gr, *Gigaspora rosea*; Gm, *Gigaspora margarita* Lb, *Laccaria bicolor*; Nc, *Neurospora crassa*; Pi, *Piriformospora indica*; Pg, *Puccinia graminis*; Os, *Oryza sativa*; Rp, *Racocetra persica*; Rc, *Rhizophagus cerebriforme*; Rcl, *Rhizophagus clarus*; Rd, *Rhizophagus diaphanous*; Ri, *Rhizophagus irregularis*; Ro, *Rhizopus oryzae*; Sc, *Saccharomyces cerevisiae*; Sl, *Suillus luteus*; Tm, *Tuber melanosporum*; Um, *Ustilago maydis*; Zm: *Zea mays.*

Fig. 4. Functional analysis of RiCRD1 in metal hypersensitive yeast mutants. The *Saccharomyces cerevisiae cup1Δ* and *yap1Δ* mutants were transformed with the empty vector or expressing *RiCRD1* and plated on SD media supplemented or not with 75µM and 2 mM $CuSO_4$, respectively. Plates were incubated 5 days at 30 ºC.

Fig. 5. Effect of high concentrations of Cu and Cd on *RiCRD1* transcript level in ERM. *R. irregularis* ERM was grown in monoxenic cultures in M-C medium (control) or in M-C medium supplemented with 250 µM $CuSO_4$, 500 µM $CuSO_4$ (A) or with 45 µM $CdSO_4$ (B) and incubated at 24°C. The time of Cu or Cd addition was referred as time 0. Mycelia were collected 1, 2 and 7 days after Cu addition and 1, 3, 6, 12, 24 and 48 hours after Cd supplementation. Some blue spores indicative of Cu compartmentalization (pointed with blue arrows) were observed 2 days after Cu addition to the ERM; images were captured under a binocular microscope just before the collect of the ERM subjected to the different Cu treatments (Scale bar: 500 μm).

RiCRD1 transcript levels were calculated by the $2^{-\Delta\Delta CT}$ method using *RiEF1α* as a normalizer. Bars represent standard error; different letters indicate statistically

1061 significant differences between treatments at the level of 0.05 according to the Tukey's
1062 b-test.

1063 **Fig. 6.** Effect of high concentrations of Cu and Cd on the transcript levels of metal
1064 tolerance related genes of *R. irregularis*. ERM was grown in monoxenic cultures in M-
1065 C medium (control) or in M-C medium supplemented with 250 µM $CuSO_4$, 500 µM
1066 $CuSO_4$ or 45 µM $CdSO_4$ and incubated at 24°C. The time of Cu or Cd addition was
1067 referred as time 0. Mycelia were collected 1, 2 and 7 days after Cu addition and 1, 3, 6,
1068 12, 24 and 48 hours after Cd supplementation. Transcripts levels of (A-B) *RiMT1*, (C-
1069 D) *RiABC1*, and (E-F) *RiPCS* were calculated by the $2^{-\Delta\Delta CT}$ method using *RiEF1α* as a
1070 normalizer. Bars represent standard error; different letters indicate statistically
1071 significant differences between treatments at the level of 0.05 according to the Tukey's
1072 b-test.

1073 **Fig. 7.** *RiCRD1* transcript levels in the *R. irregularis* ERM and IRM. Transcript levels
1074 of *RiCRD1* (A) and *RiMST2* (B) were measured in the extraradical mycelia (ERM) and
1075 the intrarradical mycelia (IRM) of *R. irregularis* grown under control conditions in
1076 monoxenic cultures (i) in the presence of T-DNA transformed carrot roots (*in vitro*
1077 system) or (ii) in the whole plant bidimensional experimental system with chicory
1078 plants (*in vivo* system). Relative transcript levels were calculated by the $2^{-\Delta\Delta CT}$ method
1079 using *RiEF1α* as a normalizer. The transcript level measured in the ERM was
1080 designated as 1. Bars represent standard error; * statistically significant differences at
1081 the level of 0.05 according to the Student's t-test.

1082 **Fig. 8.** Localization of *RiCRD1* transcripts by *in situ* hybridization in tomato roots (*L.*
1083 *esculentum* cv. Moneymaker) 8 weeks after mycorrhization with *R. irregularis*. (A-B)
1084 Trypan blue staining of roots showing root anatomy and arbuscules at two
1085 magnifications (C-F) Four repeats of the hybridization with the *RiCRD1* antisense probe

showing a specific blue staining in arbuscules. (G-H) Two repeats of the hybridization with the *RiCRD1* sense probe, in which only a weak background signal was detected. a: arbuscles (see red arrows), c: cortical cells, v: vascular tissues. Scale bars represent 20 µm.

Fig. 9. Effect of Cu deficiency on *RiCRD1* transcript levels in the IRM. *R. irregularis* colonized roots were grown in presence and in the absence of Cu in two experimental systems. Mycorrhizal carrot roots were grown in monoxenic cultures in M media (control, 0.5 µM Cu) or in M media lacking Cu (*in vitro* system) and mycorrhizal chicory roots were grown in the whole plant bidimensional experimental system (*in vivo* sandwich system) fertilized with half-strength Hoagland solution (control, 0.16 µM Cu) or with a modified nutrient solution without Cu. *RiCRD1* transcript levels were calculated by the $2^{-\Delta\Delta CT}$ method using *RiEF1α* as a normalizer. Bars represent standard error; * statistically significant differences in comparison to the control value at the level of 0.05 according to the Student's t-test.

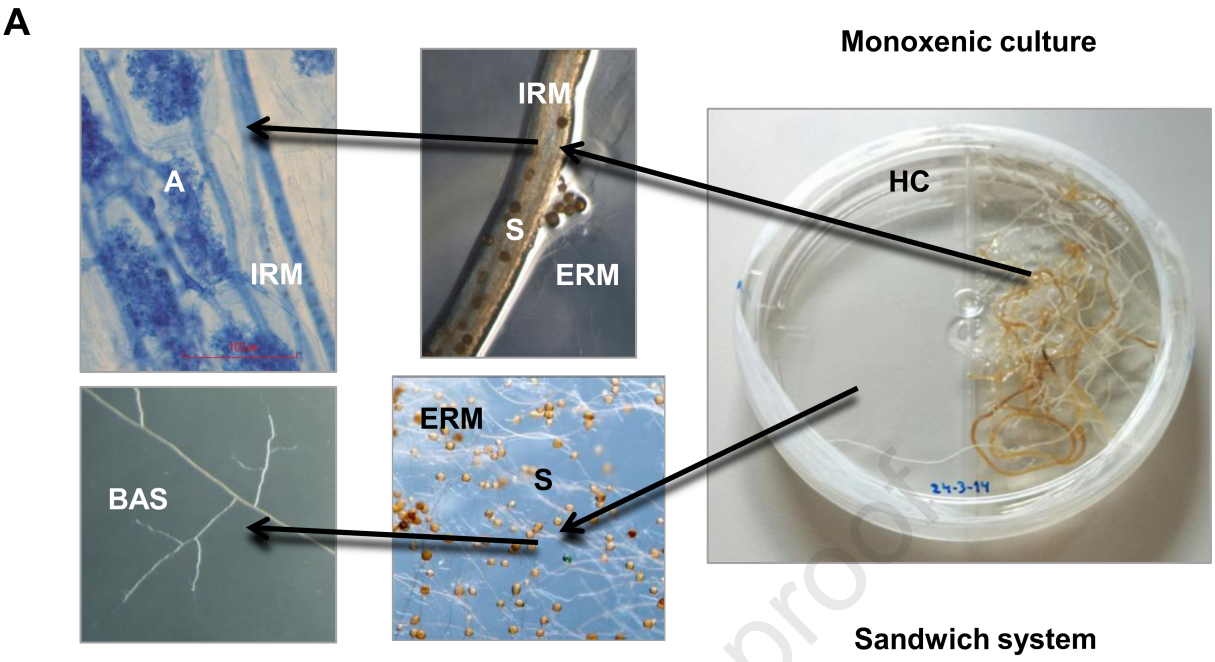

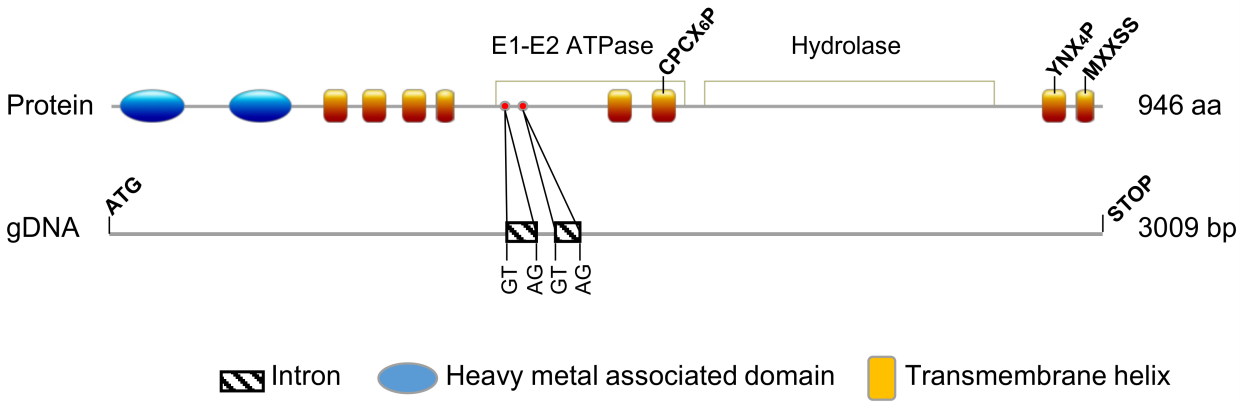

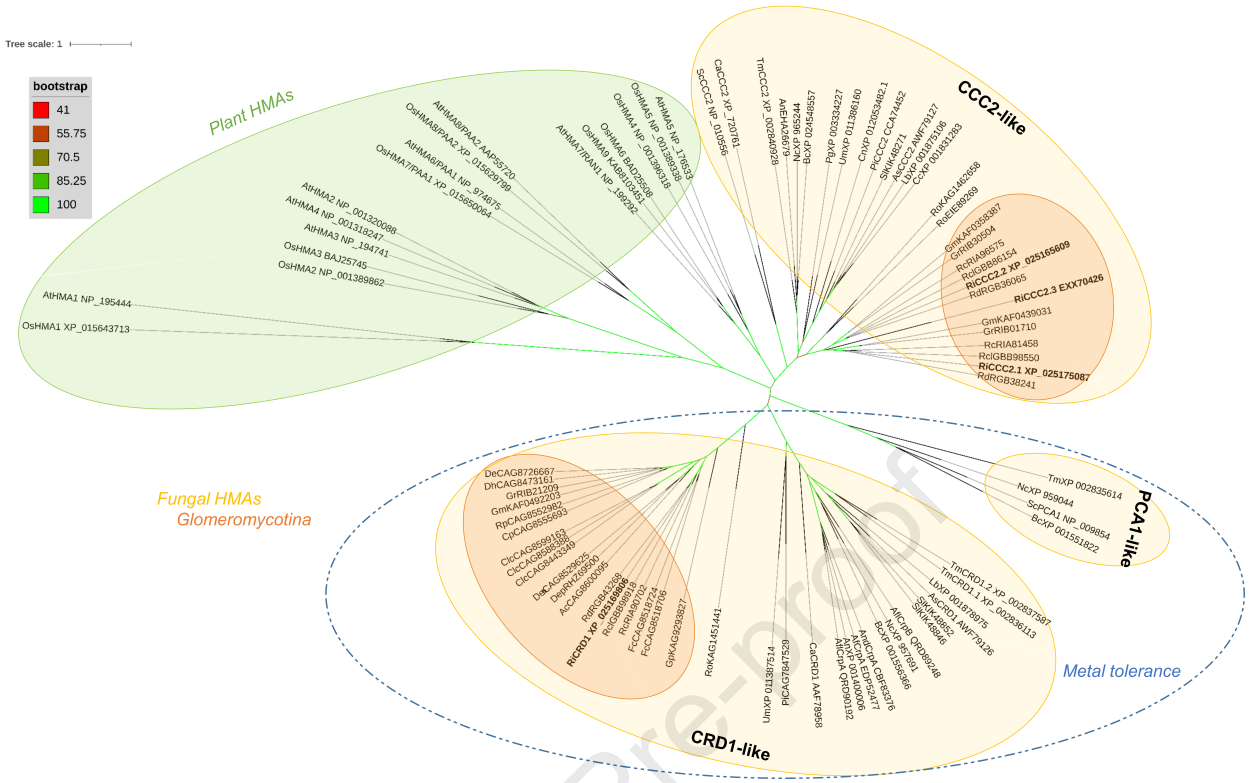

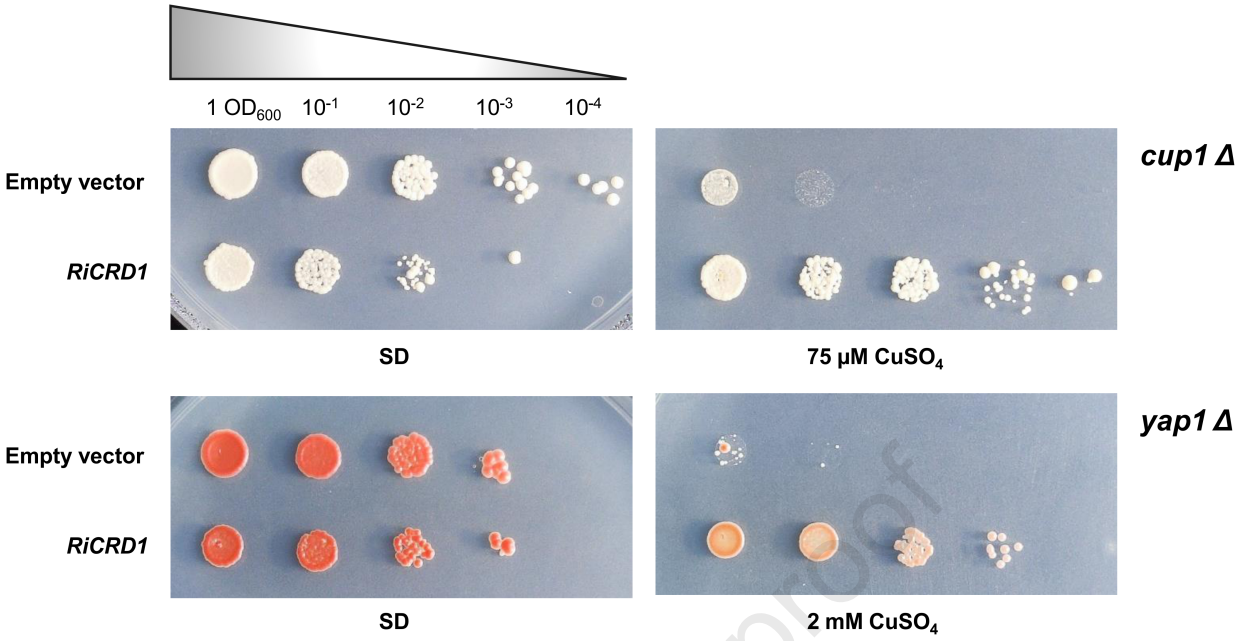

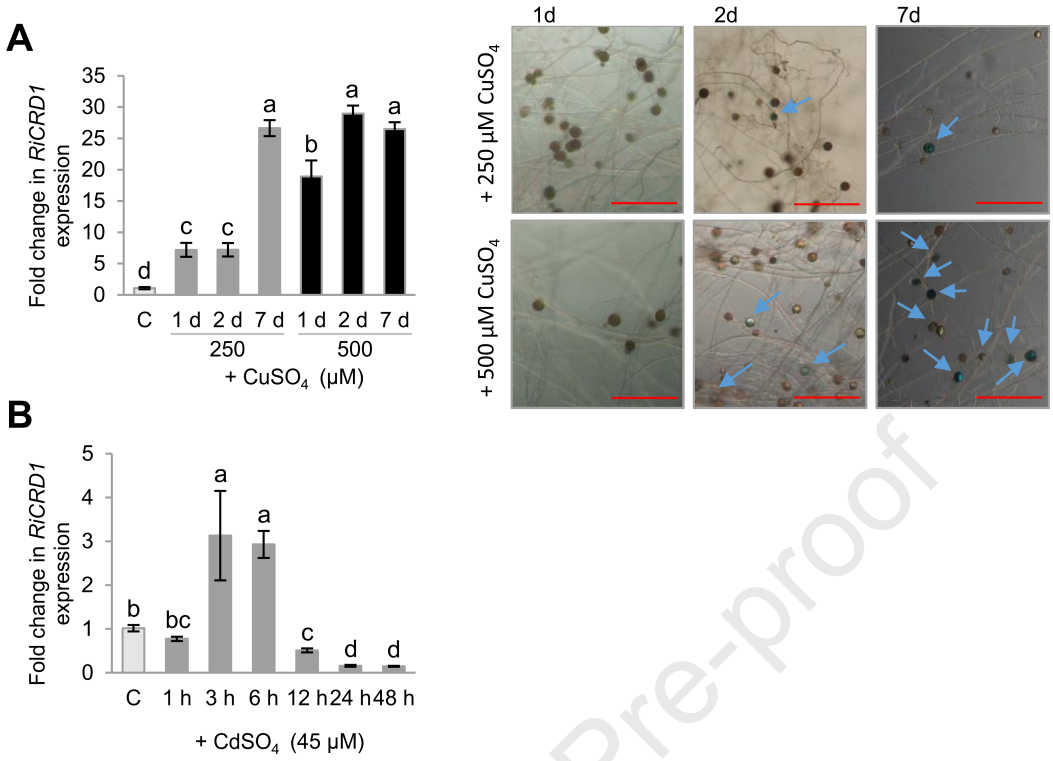

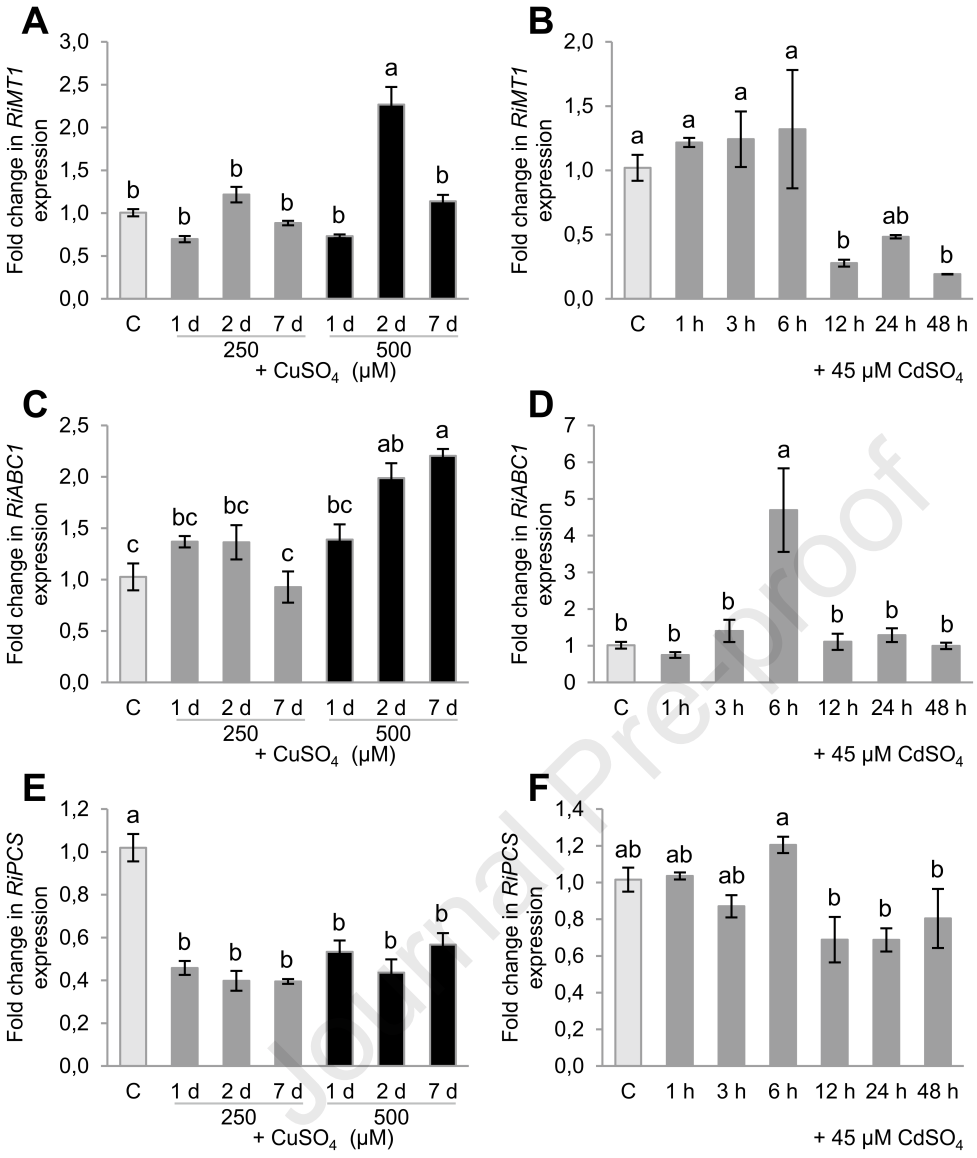

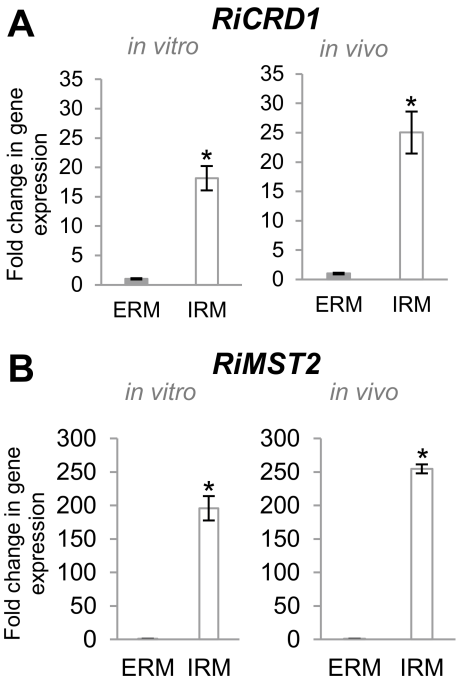

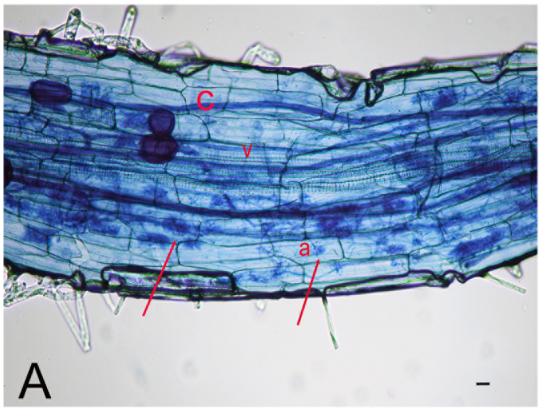
c
v
a
A

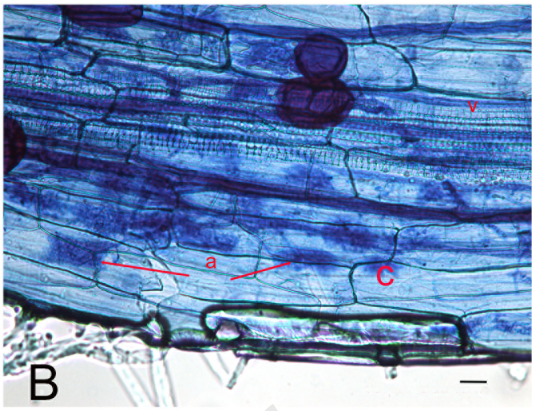
v
a
c
B

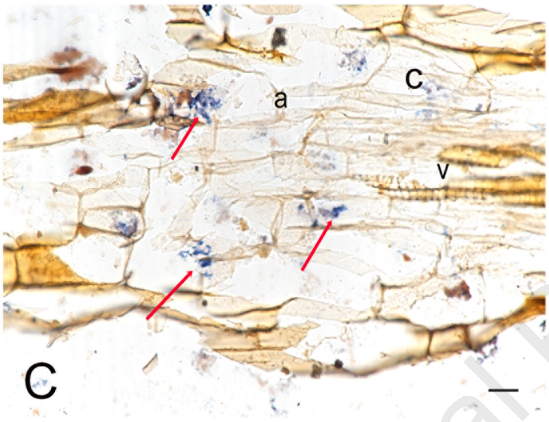
a
c
v
C

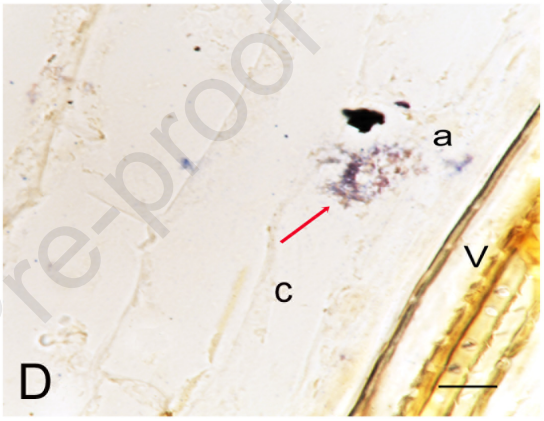
a
c
V
D

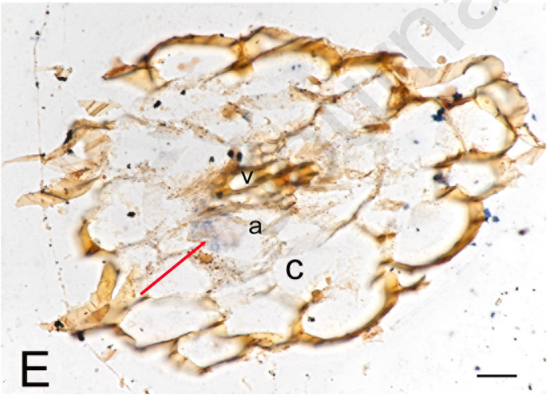
v
a
c
E

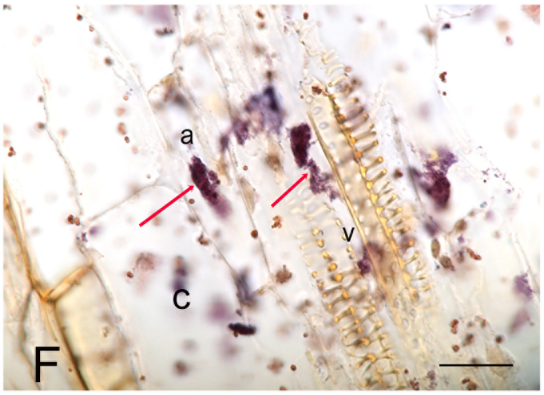
a
v
c
F

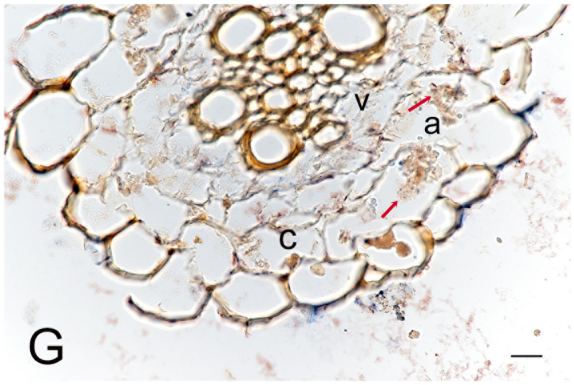
v
a
c
G

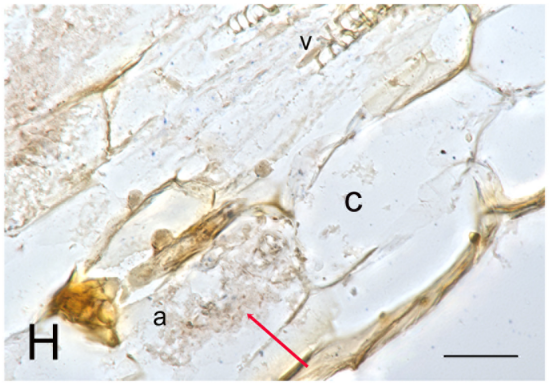
v
c
a
H

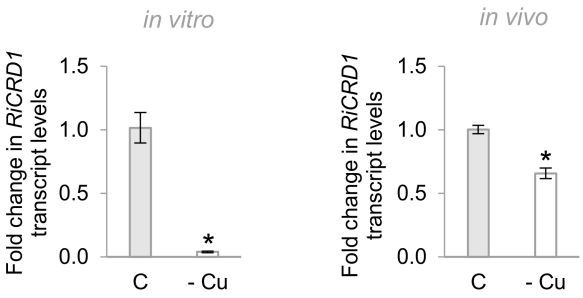

- *RiCRD1* encodes a Cu exporting ATPase in *Rhizophagus irregularis*
- RiCRD1 could play a dual role in Cu detoxification and symbiotic Cu nutrition
- *R. irregularis* mainly uses a metal efflux strategy to cope with metal toxicity

Author statement

Tamara Gómez-Gallego: Conceptualization, Methodology, Formal analysis, Investigation, Writing – original draft & editing. **Mª Jesús Molina-Luzón**: Methodology & Investigation. **Genevieve Conéjéro**: Methodology, Supervision, Writing – review & editing. **Pierre Berthomieu**: Methodology, Supervision, Writing – review & editing. **Nuria Ferrol**: Conceptualization, Methodology, Supervision, Funding acquisition, Project administration, Writing – original draft & editing.

Declaration of interests

☒ The authors declare that they have no known competing financial interests or personal relationships that could have appeared to influence the work reported in this paper.

☐ The authors declare the following financial interests/personal relationships which may be considered as potential competing interests: